



Brexit news propagation in financial systems: multidimensional visibility networks for market volatility dynamics

Maria Elena De Giuli, Andrea Flori, Daniela Lazzari & Alessandro Spelta

To cite this article: Maria Elena De Giuli, Andrea Flori, Daniela Lazzari & Alessandro Spelta (2022) Brexit news propagation in financial systems: multidimensional visibility networks for market volatility dynamics, *Quantitative Finance*, 22:5, 973-995, DOI: [10.1080/14697688.2021.1970212](https://doi.org/10.1080/14697688.2021.1970212)

To link to this article: <https://doi.org/10.1080/14697688.2021.1970212>



Published online: 14 Oct 2021.



Submit your article to this journal [↗](#)



Article views: 370



View related articles [↗](#)



View Crossmark data [↗](#)



Citing articles: 5 View citing articles [↗](#)

Brexit news propagation in financial systems: multidimensional visibility networks for market volatility dynamics

MARIA ELENA DE GIULI [†], ANDREA FLORI[‡], DANIELA LAZZARI[†] and ALESSANDRO SPELTA^{*†}

[†]Department of Economics and Management, Pavia University, Pavia 27100, Italy

[‡]Department of Management, Economics and Industrial Engineering, Politecnico di Milano, Milan 20156, Italy

(Received 2 November 2020; accepted 13 August 2021; published online 14 October 2021)

In this paper, we propose a multivariate procedure based on multidimensional visibility graphs to detect changes in the market volatility of UK financial indices, considered both before and after Brexit main events. We produce a graph-theoretical representation of volatility time series derived from equity indexes, government rates and currencies to investigate the behavior of the aggregate market volatility through the use of global centrality measures. By employing a stylized agent-based model, we show that the proposed approach is able to discriminate between periods of high and low volatility, both in the temporal dimension and cross-sectionally among multiple time series. We aim at recognizing whether external news related to the Brexit process could induce significant ‘after-shocks’ (and also ‘pre-shocks’) in the system, by producing dynamic relaxation in the values of centrality measures, in line with the cascade effects described by the Omori earthquake law. In particular, high volatility cascades dissipate into the market via power-law relaxation. When compared with other categories of events, such as Bank of England monetary policy announcements, we observe significant market inefficiency in processing Brexit related news. We also find that strong market surprise related to specific Brexit news or a correct discount of some Brexit announcements can produce an inverse Omori law exhibiting convex relaxation.

Keywords: Brexit; Market volatility; Omori law; Multidimensional visibility network

1. Introduction

Given the economic and political significance of Brexit for UK and global markets, a granular and systematic analysis of the impact of the Brexit process on financial markets is still a missing link in the existing empirical literature. In fact, most of the studies are focused on the economic or political effects of the Brexit on the UK real economy and on its relationships with the other counterparts (see, e.g. Pain and Young 2004, Vasilopoulou 2016, Hosoe 2018, Jackson and Shepotylo 2018, Driffield and Karoglou 2019, Borghesi and Flori 2019). Indeed, the Brexit vote has dragged on demand via weaker consumption and weaker business investment. As regards consumption, it remained resilient immediately following the referendum, but then declined from early 2017, as consumers saw a deterioration in their purchasing power and a worsening in their real income, as prices were

driven higher by sterling’s depreciation. Even for business, the impact was heavily concentrated in 2017, when firms faced higher costs and the expected and wished for export boom was not seen; the value of exports from the UK did not grow faster, while the value of imports was broadly lower than in the G7 countries (see Corsetti *et al.* 2019). Overall, the real economy has been negatively impacted by higher uncertainty, with business investment, productivity and real wages stalling. The export boost, instead, was not very high, as highly specialized and high value added sectors represent the larger part of exports, with products characterized by a lower elasticity to price and evidence of limited adjustment of prices to currency depreciation.

On the other hand, only a few works investigate specifically the effects of Brexit on financial systems (see, e.g. Schiereck *et al.* 2016, Armour 2017, Belke *et al.* 2018, Li 2019). For instance, Ramiah *et al.* (2017) analyze the effect of the Brexit referendum on various sectors of the British stock market and find that this effect is likely to vary across sectors,

*Corresponding author. Email: alessandro.spelta@unipv.it

Shahzad *et al.* (2019) notice that performance of UK firms may decrease because of the Brexit process and that market reaction varies during pre- and post-referendum events, while Samitas *et al.* (2018), by focusing on the financial stability channel, show that Brexit would have adverse consequences on both the UK and EU economies, especially in the long run.

We propose to study the volatility dynamics of the domestic UK financial market before and after the main Brexit-related news through the lens of network theory. In so doing, we develop a new measure inspired by visibility algorithms (see Lacasa and Flanagan 2015) and tensor decomposition (see Spelta 2017, Pecora and Spelta 2017, Spelta *et al.* 2018) to investigate the reaction of capital markets to Brexit announcements. In particular, we assess the impact of Brexit-related events on the volatility time series derived from equity indexes, government rates and currencies, which are jointly considered to describe the UK financial system from an aggregate perspective.

In recent decades time series analysis has received inputs from different disciplines, such as nonlinear dynamics, statistical physics, and Bayesian statistics. As a result, new approaches like nonlinear time series analysis grounded on algorithms, multifractal spectra and projection theorems have emerged in the literature to allow more complex investigations in several applied economic contexts (Kantz and Schreiber 2004, Hastie *et al.* 2009). Against this background, visibility algorithms have been shown to be relatively simple and analytically tractable methods for extracting nontrivial information on the original signals by providing a clean description of low dimensional dynamics (Lacasa and Flanagan 2015). In fact, visibility algorithms constitute a family of methods for mapping the information encoded in time series into a graph-based representation which embeds several properties of the original series into the topological structure of the graph. For instance, periodic series can be conveniently mapped into regular graphs, random series into random graphs, while fractal series can be represented as scale-free networks. Such information can then be effectively exploited to describe, in graph-theoretical terms, the behavior of the time series and their underlying dynamical properties (see, e.g. Zhang and Small 2006, Xu *et al.* 2008, Lacasa *et al.* 2008, Shirazi *et al.* 2009, Strozzi *et al.* 2009, Haraguchi *et al.* 2009, Donner *et al.* 2010, 2011, Campanharo *et al.* 2011, Stephen *et al.* 2015, Lacasa and Flanagan 2015, Lacasa *et al.* 2015). By representing a time series as a graph, one can therefore investigate through topological analysis the inherited structural patterns at different time scales from microscopic to macroscopic levels (Lacasa *et al.* 2008). For this reason, visibility algorithms are thus emerging as an instrumental approach, especially when dealing with nonlinearities and complexity.

In this paper, we first revise the notion of visibility graph to convert financial series into a network. Given a time series, each time-stamp is considered to be a node. Two nodes are connected by an edge if the corresponding observations are ‘visible’ from each other, i.e. if there exists a straight line connecting data values at these points and not intersecting the height of any other intermediate observations. Hence, nodes that have the highest visibility tend to show the largest numbers of edges connected to them. In other words, time stamps

associated with peaks generally present higher probabilities to connect to many other points in the series since they do not have obstacles in visibility thanks to their higher positions in the series. However, it could be also the case that local maxima create barriers between lower points and other peaks. More generally, this approach allows us to describe time observations according to their centrality levels. Most central time stamps, namely nodes with higher visibility, can thus be interpreted as critical points in the series since they identify moments where volatility deviates substantially from its long-run behavior.

Given such visibility graph representation for volatility patterns of different financial assets over time, we then apply a probabilistic tensor decomposition (Kolda *et al.* 2005, Kolda and Bader 2009) to obtain global centrality measures from the resulting visibility multi-layer network. This procedure allows us to synthesize the volatility behaviors of the series, both in time and cross-sectionally, through a global measure that we call *Multidimensional Volatility Indicator (MVI)*. In practice, *MVI* simultaneously considers the induced visibility both in the temporal and cross-sectional dimensions, together with their feedback mechanisms. Moreover, such tensor decomposition also provides an additional score, which we call *Type Centrality (TC)*, expressing the contribution of each asset series to determine the centrality scores of time nodes.

Multi-layer financial networks have been recently employed to describe multidimensional inter-linkages between economic agents (see Poledna *et al.* 2015, Montagna and Kok 2016, Aldasoro and Alves 2018), especially in the context of interbank lending. However, the existing literature mainly focuses on creating an aggregate network representation by summing over single networks, thus failing to adequately capture nonlinearities generated by the multi-layered nature of the data (Gauvin *et al.* 2014). In this paper, we extend the approach proposed by Avdjiev *et al.* (2019) for international bank lending to a visibility multi-layer network. Differently from the multi-layer financial networks typically employed in the domain of interbank lending modeling, with nodes representing financial institutions, in our analysis nodes stand for time stamps connected by the visibility approach. Therefore, the *MVI* obtained from the visibility multi-layer network can be interpreted probabilistically in terms of the dynamics of the aggregate underlying system, taking multiple types of financial markets simultaneously into account. The higher the importance of a node, i.e. the higher the *MVI* in that time stamp, the greater the probability that a consistent number of asset series display co-movements during high volatility periods, meaning that in such time stamps these series show substantial deviations from ‘business as usual’ dynamics. This approach is parameter free and does not require any assumption on the functional form of the data generating process, allowing us to study even non-stationary time series, which may present phenomena like long-range memory, and that are likely to lead to phases of market instability. Hence, the identification of a nodes centrality allows us to study relevant nonlinear properties of the underlying multilayer network, such as system synchronization. Indeed, the presence of nodes becoming very central reveals an increased synchronization of the time series, which is likely to occur when the system is far from its equilibrium

configuration. Conversely, during periods of market stability, nodal centrality is more evenly distributed, thus indicating that the system is close to equilibrium (see Lacasa *et al.* 2015). Moreover, tensor decomposition is instrumental when working with multiple networks. The resulting centralities, associated with time stamps, indicate an increasing synchronization phase of the system, thus signaling potential abrupt transitions in the behavior of the underlying system. Time periods associated with highly connected nodes in multilayer networks will be those representing spikes in most of the series, surrounded by observations with a low deviation. Hence, in our work we rely on multilayer centrality scores to uncover the emergence of such synchronized patterns between financial time series and to assess the intensity of self-organizing processes arising from market co-movements and positive feedbacks (see Heemeijer *et al.* 2009, Flori *et al.* 2019, Spelta *et al.* 2020, Flori *et al.* 2021), especially around Brexit-related announcements.

We introduce a stylized Agent-Based model to validate, in a controlled environment, the *MVI* ability to capture high and correlated volatility patterns in multiple time series. In other words, the Agent-Based model is instrumental in verifying the value added by using a multiplex visibility graph and a centrality measure computed on the temporal dimension of such a graph (namely, the *MVI*) to synthesize co-movements between different series. Agents can in fact herd towards a common strategy and lead the price to deviate from its fundamental value, causing financial crashes and volatility outbursts, to be locally either self-enforcing or dissipating. Our analysis shows how the empirically observed market volatility captured by the *MVI* can be related to agents' behaviors at micro level, whose interactions can bring larger effects at macro level to the whole financial market. This framework is very suitable for investigating the nonlinear dynamics occurring among interacting agents that populate a financial market, and that cannot be assessed only by considering aggregate variables, such as asset prices or returns.

More specifically, to analyze the dynamic response of the aggregate market volatility to exogenous shocks related to the Brexit process, we study fluctuations of the *MVI*'s distribution using concepts developed in the field of seismology (Omori 1894, Utsu 1961), deriving parallels between energy cascades and information cascades. In particular, we analyze the role that different external news plays in explaining the rate of occurrence of large volatility fluctuations in the financial system. This gives the means to study the behavior of the *MVI* associated to time points in the neighborhood of relevant external events that may have impacted on the asset price dynamics. Hence, we aim at recognizing whether news related to the Brexit process could induce significant 'after-shocks' (and also 'pre-shocks') in the system by producing dynamic relaxation in the values of the centrality measures in line with the cascade effects which follow an earthquake's energy propagation. The occurrence of an exogenous shock on a financial market may in fact increase the likelihood of other consequent shocks. In particular, several papers (see, e.g. Lillo and Mantegna 2003, 2004, Selçuk 2004, Selçuk and Gençay 2006, Weber *et al.* 2007, Petersen *et al.* 2010a, 2010b, Siokis 2012, Pagnottoni *et al.* 2021, Spelta *et al.* 2021) have shown that a power-law tail describes quite well the

dynamics of market volatility after a major financial shock. For instance, specific negative events have been studied by Sornette *et al.* (1996) and Lillo and Mantegna (2003, 2004) who analyzed the volatility dissipation before and after the Black Monday crash in 1987 and found evidence of a power-law decay rate coherent with the Omori law. The role of announcements has been instead reported in Petersen *et al.* (2010a), who found that FED announcements regarding interest rate changes produce volatility outbursts decaying in line with the Omori law, while a comparison of estimated Omori exponents for different financial indices is reported in Selçuk (2004) for emerging markets. In our framework, the Omori law, which describes the non-stationary phase observed after a big earthquake, turns out to be instrumental in describing the dynamical response of a financial system when it is pushed far away from its equilibrium state due to the occurrence of an extreme event.

Our analysis reveals that Brexit announcements produce financial shocks whose dynamics can be described by an analogue of the Omori earthquake law. Indeed, we find that the Brexit process induces high volatility cascades of 'after-shocks', which follow power-law decay, here interpreted as market inefficiency in processing the events. We also notice that the same law describes 'pre-shock' behavior before the date of the Brexit events. Moreover, the UK financial system shows a different degree of reaction to the events affecting the British markets. We observe significant market inefficiency in processing Brexit related news, in particular if compared to other categories of events, such as Bank of England monetary policy announcements and policy actions. We also find that in some cases Brexit announcements produce an inverse Omori law exhibiting convex relaxation due to strong market surprise or a correct discount of Brexit news.

The paper is composed as follows: Section 2 presents the data set employed in the paper together with the methodology. In particular, in Sections 2.1, 2.2 and 2.3, we present the visibility algorithm used to convert time series into networks, the tensor decomposition used to extract centrality measures and the study of such topological measures through the Omori earthquake law, respectively. Section 3 gives the results and discusses a simplified agent-based model to describe how our proposed approach can discriminate between periods of high and low volatility across multiple time series. Section 4 concludes.

2. Data and methodology

The Brexit process has stormed the global financial market inducing significant perturbation in asset prices, which we analyze from a multidimensional perspective. We study the behavior of the *MVI* in the neighborhood of relevant events potentially affecting market dynamics to investigate the role that different news play in explaining the rate of occurrence of large fluctuations in the financial system. To better understand aggregate market responses on different types of shocks, we classify relevant external news observed in the markets over the 3-year period 2016–2019 into two different categories, namely: news regarding Brexit events and monetary policy ones.

We consider the following variables grouped in asset classes. The asset class equity is represented by the FTSE UK Indexes that measures the performance of all capital and industry segments of the UK equity market, therefore from large cap to small cap companies: FTSE100 (UKXIndex), FTSE250 (MCXIndex), FTSE350 (NMXIndex), FTSE All-Share (ASXIndex), FTSE Techmark Focus (T1XIndex), FTSE AIM All-Share Index (AXXIndex), FTSE Small Capitalization Index (SMXIndex). The UK government yield curve is represented by 2, 5, 10, 30 yearly maturities (GTGBP2YCorp, GTGBP5YCorp, GTGBP10YCorp, GTGBP30YCorp). Finally, we consider the sterling (GBP) cross rates against the main currencies, i.e. US dollar (USBPCurrency), Euro (BPEUCurrency), Yen (JYBPCurrency) and Swiss Franc (SFBPCurrency). The daily observations (from January 2016 to November 2019) are obtained from the Bloomberg database.† All values are expressed in GBP and, for each asset, we compute the daily volatility dynamics as the absolute value of the asset return (see Weber *et al.* 2007, Petersen *et al.* 2010a, 2010b, Nowak *et al.* 2011).

2.1. Natural visibility graph

To build up networks from assets' time series, we follow Lacasa *et al.* (2008) who propose to transform a time series into a graph or network according to a mapping algorithm named Natural Visibility, which links every point of the time series with all those that can be 'seen' from the top of the considered point. In the resulting graph, every node corresponds to a time stamp in the time series and two nodes are connected if they are visible from each other, i.e. if there exists a straight line connecting such pair of nodes, provided that this line does not intersect the height of any other intermediate point. This method produces an undirected graph, invariant under affine transformations of the series, where nodes with high centrality scores are the time points most connected with the rest of the graph (see Lacasa and Flanagan 2015).

Formally, the following criterion establishes how edges connecting time stamps are created, thus constituting the backbone of the visibility graph. Two time stamps, t_a and t_b , of a series whose corresponding values are y_a and y_b , will represent connected nodes of the associated visibility graph, i.e. $V(a, b) = 1$, if any other data (t_c, y_c) placed between them fulfills the following inequality condition:

$$V(a, b) = 1 \quad \text{if} \quad y_c < y_b + (y_a - y_b) \frac{t_b - t_c}{t_b - t_a} \quad (1)$$

Such graph-theoretical algorithms are typically exploited to extract in a simple and parsimonious way the relevant information on the dynamics of an underlying system (Lacasa *et al.* 2008, Xu *et al.* 2008, Lacasa *et al.* 2009, Donner *et al.* 2011, Gonçalves *et al.* 2016). In particular, visibility graphs have been largely devoted to the analysis of univariate time series (exceptions are Lacasa *et al.* 2015 and Flori *et al.* 2021), while their capability to detect quantitative early warnings signals of financial crisis and local instabilities (see,

e.g. Serafino *et al.* 2017) make them suitable for the study of financial distress. In order to assess the contribution of different asset classes to market instability, we then propose a tensorial approach to visibility graphs to simultaneously address both the cross-sectional and time dimensions, in a way that multiple time series are jointly considered.

2.2. Tensor decomposition and centrality measures

The probabilistic tensor decomposition results in two centrality scores (Kleinberg 1999, Kolda *et al.* 2005, Kolda and Bader 2009), namely: the Multidimensional Volatility Indicator (*MVI*) and the Type Centrality (*TC*). These scores are associated respectively to the temporal and to the cross-sectional dimension of the multi-layer network. While the first indicates the importance of each time point in terms of magnitude and co-movement among the series, the second contains information on the probability that high scoring nodes are connected in such layer, i.e. it reveals information on whether time points with high values of the Multidimensional Volatility Indicator see each other in that particular time series thus contributing to the centrality of the time stamps that are connected on such layer.

Formally, following Kolda and Bader (2009) a third-order tensor is an element of the tensor product of 3-vector spaces, each of which has its own coordinate system. The multi-layer network, in which each layer represents a visibility graph associated with one of the K time series of length T , can thus be mapped into a third-order tensor $\mathcal{V} \in \mathbb{R}^{T \times T \times K}$, as we have a two-dimensional visibility graph for each asset series $k \in K$, the latter representing the third dimension. Hence, $\mathcal{V} \in \mathbb{R}^{T \times T \times K}$ represents a three-order tensor obtained by stacking the adjacency matrices of the visibility graphs V_k for $k = 1, \dots, K$. Each element of the tensor v_{ijk} takes value 1 if nodes i and nodes j are connected in the k th layer, and zeros otherwise.

The TOPHITS algorithm was developed by Kolda *et al.* (2005) as a generalization of the HITS algorithm (Kleinberg 1999) for multidimensional arrays. In our framework, it provides a global centrality measure for nodes, i.e. time stamps, and layers, i.e. price time series, by determining one score for each dimension of the tensor. In order to get centrality measures with a probabilistic interpretation, we rely on a modification of the TOPHITS algorithm following Ng *et al.* (2011) and we consider a Markov chain on the tensor, whose joint stationary distribution will be the product of the centrality measures *MVI* and *TC*.

To obtain the centrality measures from the visibility multi-layer network, the starting point is the computation of the (bivariate) conditional frequencies \mathcal{H} and \mathcal{R} for time stamps and asset types, respectively. These scores can be obtained by normalizing the entries of the tensor \mathcal{V} as follows:

$$\begin{aligned} h_{i|jk} &= \frac{v_{ijk}}{\sum_{i=1}^T v_{ijk}} \quad i = 1, \dots, T \\ r_{k|ij} &= \frac{v_{ijk}}{\sum_{k=1}^K v_{ijk}} \quad k = 1, \dots, K \end{aligned} \quad (2)$$

being $h_{i|jk}$ the probability of visiting the i th node given that the j th node is currently visited using the k th layer and being $r_{k|ij}$

† In parenthesis, the financial indices labels retrieved from Bloomberg website.

the probability of using the k th layer given that the j th node is visited from the i th node. We account for the so-called dead ends nodes when $v_{ijk} = 0$ by setting the values of h_{ijk} equal to $1/T$ and the value of r_{kij} to $1/K$.

The above quantities can be used to estimate the conditional probabilities:

$$\begin{aligned} Pr[X_\eta = i | X_\eta = j, Z_\eta = k] \\ Pr[Z_\eta = k | X_\eta = i, X_\eta = j] \end{aligned} \quad (3)$$

where random variables X_η and Z_η stand for the visit of any particular node using any asset type, at the step η of the Markov chain.

The conditional frequencies can be used to derive the stationary marginal probabilities:

$$\begin{aligned} Pr[X_\eta = i] &= \sum_{j=1}^T \sum_{k=1}^K h_{ijk} Pr[X_\eta = j, Z_\eta = k] \\ Pr[Z_\eta = k] &= \sum_{i=1}^T \sum_{j=1}^T r_{kij} Pr[X_\eta = i, X_\eta = j] \end{aligned} \quad (4)$$

whose limiting distributions can be used to compute MVI and TC as follows:

$$\begin{aligned} MVI_i &= \lim_{\eta \rightarrow \infty} Pr[X_\eta = i] \\ TC_k &= \lim_{\eta \rightarrow \infty} Pr[Z_\eta = k] \end{aligned} \quad (5)$$

Finally, in line with the TOPHITS algorithm, the centralities can be computed iteratively solving the following system of equations:

$$\begin{aligned} MVI_i &= \sum_{j=1}^T \sum_{k=1}^K h_{ijk} MVI_j TC_k \quad i = 1, \dots, T \\ TC_k &= \sum_{i=1}^T \sum_{j=1}^T r_{kij} MVI_i MVI_j \quad k = 1, \dots, K \end{aligned} \quad (6)$$

In a word, let K denote the total number of asset series for which a visibility graph V_k is computed and let TC_k be the score corresponding to the importance of the k th series, i.e. the contribution of the k th series to the importance of the nodes in the visibility tensor. Moreover, let MVI_i and MVI_j be the scores corresponding to the importance of the i th and j th nodes, i.e. the importance of the i th (j th) time point across multiple series in terms of visibility.

The centrality score MVI_i related to the importance of the i th node (or time point) is the weighted sum of the centrality scores MVI_j of the nodes that are ‘visible’ from i along all the asset series. The weight associated with each visible node j is the product of the element of the transition probability tensor \mathcal{H} between the pair of nodes (i, j) multiplied by the type score TC_k of the layer in which the link is present.

The type centrality score of layer k (namely, TC_k) is the sum, over all pairs of nodes (i, j) connected in layer k , of the product between their centrality score MVI_i and MVI_j with

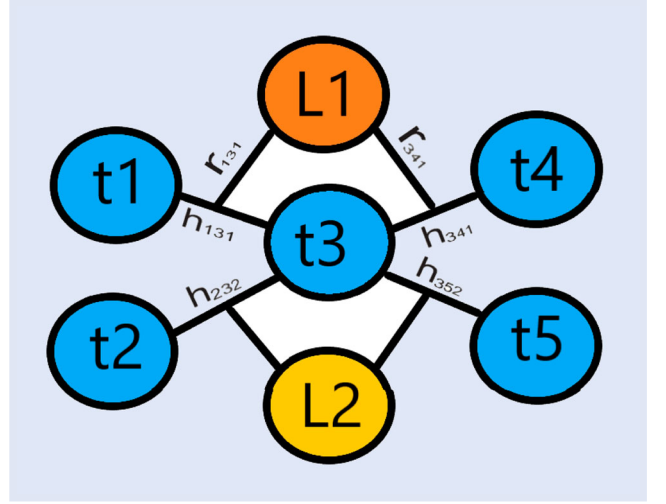


Figure 1. *Multi-layer network example and MVI , TC computations*: the network has two layers, L1 (the stock layer for instance) and L2 (suppose the exchange rate layer), and five time stamps (nodes created with the visibility algorithm). In L1, the time stamp $t3$ is connected to $t1$ with probability h_{131} and to $t4$ with probability h_{341} . In L2, $t3$ is connected to $t2$ and $t5$ with probabilities h_{232} and h_{352} , respectively. For instance, the MVI associated to time stamp $t3$ is thus $MVI_{t3} = MV_{I_1} h_{131} TC_{L1} + MV_{I_4} h_{341} TC_{L1} + MV_{I_2} h_{232} TC_{L2} + MV_{I_5} h_{352} TC_{L2}$, while the TC of L1 is: $TC_{L1} = MV_{I_1} MV_{I_3} r_{131} + MV_{I_4} MV_{I_3} r_{341}$.

the element of the transition probability tensor \mathcal{R} between i and j .

The tensor decomposition is closely linked to Correspondence Analysis, which is a standard multivariate statistical technique employed to analyze frequency tables. In a nutshell, in Correspondence Analysis, a frequency table represents the number of occurrences of cases having both values ‘ x ’ for the row variable and ‘ y ’ for the column variable. Correspondence Analysis creates a score to the values of each of these variables. These scores link the two variables with a reciprocal averaging relation. In our case, for each network layer, the records are the edges founded by the application of the visibility algorithm, and the system of equation (6) design the reciprocal averaging relation. Moreover, figure 1 illustrates the computation of the MVI and TC scores on a multiplex to help the understanding of the key elements of the multi-layer network tensor decomposition.

2.3. Visibility cascading dynamics

Perturbations in asset prices due to exogenous shocks are a topic of study for economists, mathematicians, and physicists (see, e.g. Fama 1965, Ding *et al.* 1993, Mandelbrot 1997, Mantegna and Stanley 1999, among others). Here, common patterns of complex interactions, derived from the topology of the visibility graphs and extracted via tensor decomposition, are used to investigate the impact of external shocks on the volatility of the aggregate financial system and to assess how the dynamics of the system changes relatively to different types of shocks affecting such system. More specifically, we analyze the role that different news play in explaining the rate of occurrence of large fluctuations in the UK financial

system. This means to investigate the behavior of the MVI in the neighborhood of relevant events that might affect market dynamics. To better understand aggregate market responses to different types of shocks, we classify relevant external news observed in the markets over the 3-year period 2016–2019 into two different categories, namely: news regarding the Brexit events and monetary policy ones.

Then, the Omori law helps us in quantifying how the after-shocks (or pre-shocks) aggregate market conditions synthesized by MVI decay with time. For each type of external shock, we thus investigate whether the behavior of MVI in the 10 trading days interval following (and proceeding) the day of the news fulfills the so-called Omori law. In other words, we investigate the system dynamics around the neighborhood of the day of each event to assess the laws governing the behavior of MVI . It is worth noting that in this framework the pre-shocks estimated Omori exponents cannot be interpreted as forecasting properties for the corresponding impact of the main shock. However, the statistical regularity found for a specific financial market, before and after a market shock, could be exploited for instance to estimate the time window over which after-shocks can be expected. This is also related to the ability of processing information that may anticipate or follow an external shock, such as a specific type of announcement. The frequency of cascades, as well as the estimate of the end time of such market dynamics, could be viewed as a desirable state for processing information. Hence, by fitting the data by the Omori law with estimated parameters, it is then possible to estimate how long the relaxation process will take and how large effects it will bring under the hypothesis of a power-law decay.

In order to study the aggregate market dynamics around an external shock occurring at time T_s , we analyze the daily variation $MVI(|t - T_s|)$ around time T_s . $MVI(|t - T_s|)$ quantifies the value of the centrality measure at time t both before and after a market shock occurring at time T_s . Specifically, the Omori law describes the dynamics of this measure following a perturbation at time T_s as

$$MVI(|t - T_s|) \sim |t - T_s|^{\beta_{MVI}} \quad (7)$$

where the parameters β_{MVI} stands for the Omori power-law exponent, $t < T_s$ corresponds to the period before the main shock, and $t > T_s$ corresponds to the dynamics after the main shock. In the analysis that follows, we focus on $CMVI(|t - T_s|)$, which represents the cumulative value of the Multivariate Volatility Indicator during the period $|t - T_s|$, namely:

$$CMVI(|t - T_s|) = \int_{T_s}^t MVI(|t' - T_s|) dt' \equiv \alpha_{MVI} (|t - T_s|)^{1 - \beta_{MVI}} \quad (8)$$

Finally, to compare the visibility dynamics before and after the news-related event, we separate centrality values symmetrically around T_s as $CMVI_b(t|t < T_s)$ and $CMVI_a(t|t > T_s)$, where suffixes b and a stand for before and after shock periods, respectively. We define the displaced time as $\tau = |t - T_s|$. Then, we employ a linear OLS fit on a log–log scale to estimate the Omori power law exponents $\beta_{MVI,a}$ and $\beta_{MVI,b}$.

Figure 2 represents the work flow of the proposed approach which is composed by three main methodological steps. First from the price time series, we compute the daily volatility of the underlying assets. Each volatility series is then transformed into a network by means of the Natural Visibility algorithm proposed by Lacasa *et al.* 2008 (panel A). Then, a multi-layer network is obtained by staking the adjacency matrices of each layer into a single mathematical object called tensor. Tensor decomposition is applied to the generated visibility multi-layer network to extract relevant features of its relationships and build a synthetic indicator as the proposed Multidimensional Volatility Indicator (panel B). Then, the statistical properties of the Multidimensional Volatility Indicator observed in the neighborhood of relevant Brexit announcements (panel C) are analyzed in order to find the functional form of the relaxation dynamics (panel D).

3. Results

3.1. A simple Agent-Based model

Before proceeding with the empirical analysis, we introduce a simplified Agent-Based model similar to Menkhoff *et al.* (2009) to show that the visibility approach together with the probabilistic tensor decomposition are instrumental for discriminating between periods of high and low volatility across multiple time series. In so doing, we aim to relate what is observed at macro-level in a financial market with a precise description of the micro-level relationships between market's participants, at the origin of the propagation of financial instability and its dissipation. We employ an Agent-Based model to describe how agents' behavior can amplify market patterns induced by shocks, such as news provision and announcements, thereby generating long-lasting volatility dynamics. Investors willing to switch towards better performing strategies, as well as their reactivity to the market changes, are in fact relevant to understand the observed market response (see Barberis *et al.* 1998). Our proposed model thus assumes that the price adjustment of the i th asset is given by the price impact function:

$$p_{t+1,i} = p_{t,i} + a(W_{t,i}^C D_{t,i}^C + W_{t,i}^F D_{t,i}^F) + \epsilon_{t,i} \quad (9)$$

where $D_{t,i}^C$ and $D_{t,i}^F$ represent the book orders generated by chartists and fundamentalists, respectively, $W_{t,i}^C$ and $W_{t,i}^F$ stand for the proportion of agents using these strategies, and a is a positive reaction parameter. Equation (9) can be interpreted as a market maker scenario, where prices are adjusted according to observed excess demand. The noise term $\epsilon_{t,i}$ is *i.i.d.* normally distributed with standard deviation σ_i and represents an exogenous shock affecting price dynamics.

Chartists expect that the direction of the recently observed price trend is going to continue, while fundamentalists expect that a fraction of the actual perceived mispricing is corrected during the next period. Assuming that the demand generated by each type of investors positively depends on the expected price development leads to

$$D_{t,i}^C = b(p_{t,i} - p_{t-1,i}) \quad (10)$$

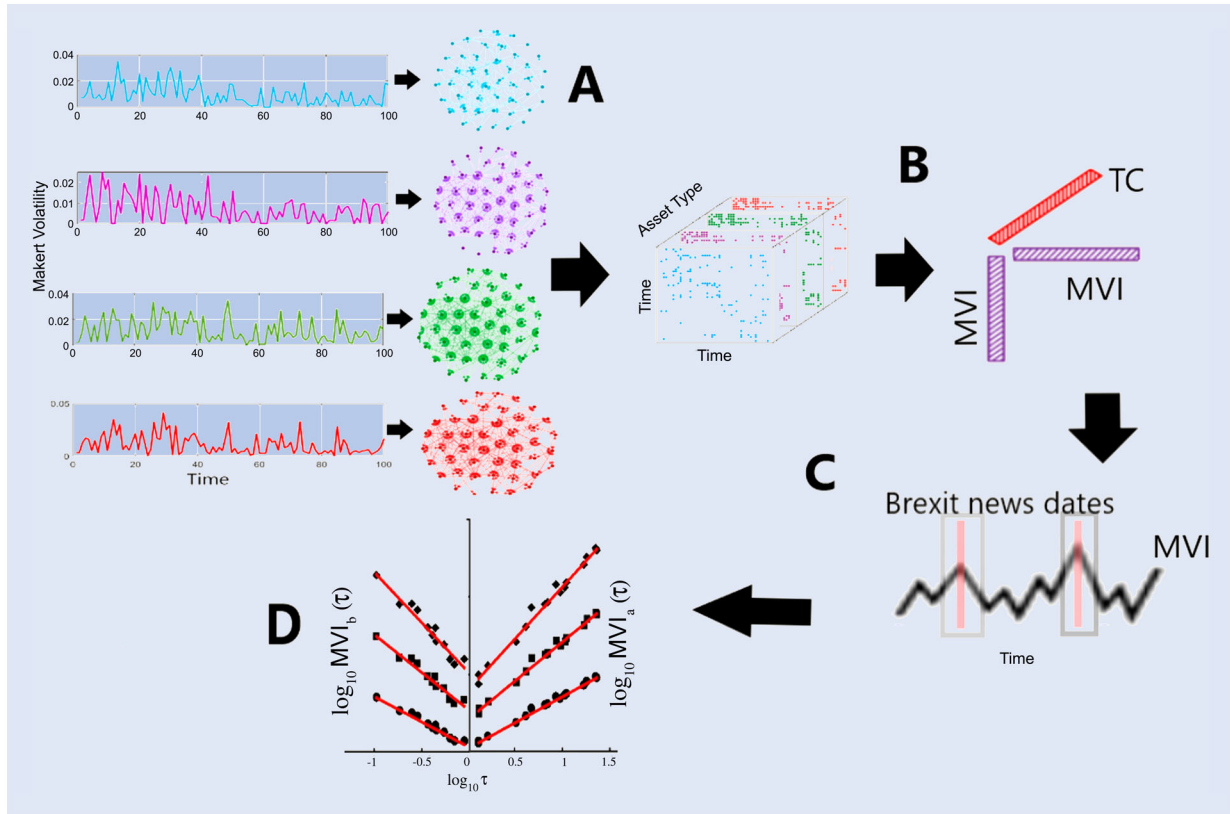


Figure 2. *Work-flow of the analysis*: the figure shows the steps introduced to investigate the impact of the Brexit process on the UK aggregate financial system. The series are transformed into a network by means of the Natural Visibility algorithm (panel A). The tensor is obtained by staking the adjacency matrices of each layer. Then tensor decomposition is applied to extract relevant features of its relationships to build MVI values (panel B). Then, the statistical properties of MVI values observed in the neighborhood of relevant Brexit announcements (panel C) are analyzed in order to find the functional form of the relaxation dynamics (panel D).

$$D_{t,i}^F = c(p_f - p_t) \quad (11)$$

where p_f is the fundamental value that we set for simplicity to be equal to zero. The fractions of agents using the two different investment strategies are not fixed over time. Agents continuously evaluate the strategies they use according to past performance. The better a strategy performs relative to the other one, the more likely it is that agents will employ it. Thus the fraction of agents that employ strategy $s = \{C, F\}$ is given by the well-known discrete choice model:

$$W_{t,i}^s = \frac{\exp(eA_{t,i}^s)}{\exp(eA_{t,i}^C) + \exp(eA_{t,i}^F)} \quad (12)$$

where $A_{t,i}^s$ is the attractiveness of a particular strategy, which depends on its most recent performance

$$A_{t,i}^s = (\exp(p_{t,i}) - \exp(p_{t-1,i}))D_{t-2,i}^s + dA_{t-1,i}^s \quad (13)$$

The memory parameter $0 \geq d \geq 1$ defines the strength with which agents discount past profits. The more attractive a strategy, the higher the fraction of agents using it. Note that the probability of choosing one of the two strategies is bounded between 0 and 1. The positive parameter e measures the intensity of choice. The higher (lower) e , the greater (smaller) the fraction of agents that will employ the strategy with the highest attractiveness. This parameter is often called the rationality parameter in Agent-Based financial market models.

To inspect the functioning of the probabilistic tensor decomposition and the visibility mapping, we propose an example based on simulated time series derived from the aforementioned simplified Agent-Based model. We illustrate the ability of the centrality measures in discriminating between time periods with low and high volatility when only one time series is considered. We show how the MVI varies as long as multiple time series co-move. Here, the exogenous component ϵ plays the role of an unexpected shock affecting the system, propagated by the chartist-fundamentalist interaction mechanism. To generate observations from the model, we use the following parametrization, $b = 0.5$, $c = 0.5$, $e = 100$, $p_f = 0$, $a = 1$ and $d = 0.5$, with $\epsilon \sim \mathcal{N}(0, 0.15)$.

Proceeding step by step, first we suppose to have only one asset ($i = 1$) and we generate 1000 time series of length $T = 200$ with different random draw for ϵ . Then, we compute the average correlation between volatility, computed as the absolute difference of price returns, and our proposed centrality measure. Notice that, for this special case, we deal with a mono-layer network since we have only one asset volatility time series. The resulting centrality measure is the two-dimensional counterpart of the MVI , which can be easily computed by letting the asset type dimension $k = 1$ in Formula 6. Second, we set $i = 2$ generating for each asset 1000 time series of length $T = 200$. In this case, we use correlated shocks playing with ϵ to show that, the more the volatility series are correlated, the higher the corresponding value of MVI .

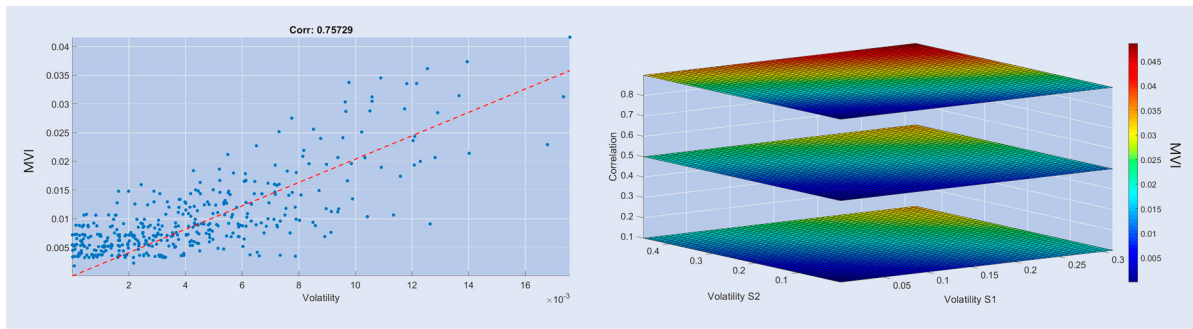


Figure 3. *Centrality measures and volatility correlation*: Figure reports results obtained from the simulative analyses. In the left panel, we show the scatter plot of the volatility associated to each time observation against the relative centrality measure of the time stamp, in the visibility network, together with the linear fit (red dashed line). In the right panel, we report results of the simulation in the case of two time series for different values of the correlation (0, 0.5, 0.99) of the exogenous component of the model. The value assumed by the *MVI* is reported in the colorbar.

Figure 3 shows, in the left panel, the scatter plot of the volatility associated to each time observation against the relative centrality measure of the time stamp computed in the visibility network, together with the linear fit (red dashed line). Correlation is positive and about 0.75, meaning that we are able to map low and high volatility periods with the two-dimensional centrality measure. Moreover, in the right panel of figure 3 we report results of the simulation in the case of two time series for different values of the correlation (0, 0.5, 0.99) of the exogenous component of the model. The value assumed by *MVI* is reported in the colorbar. Notice that the higher the volatility of the series and the higher their correlation, then the higher the value of the centrality measure. This example, therefore, is instrumental to show the ability of the proposed tensorial approach to take into account volatility behaviors both temporally and cross-sectionally. In the complex and uncertain phase due to the Brexit evolution, addressing short-term shocks in the financial system is thus not enough to address potentially severe market risks derived from it. Hence, the adoption of a stylized Agent-Based framework turns out to be relevant for understanding the micro-level behavior of investors reacting to different policy scenarios and news provision at a macro-level. In Appendix A.6, we also report the sensitivity analysis on model's parameters to show that the *MVIs* feature that we investigate in the Agent Based environment is maintained as long as model parameter changes.

3.2. An economic interpretation of financial volatility taking in Brexit announcement via the *MVI* and *TCI* indicators

The Brexit process has already had significant short-term effects on financial markets and is expected to have long-term effects on real economic activity. Figure 4, in the upper panel, shows the *MVI* behavior during the period 2016–2019 together with dashed color lines, which identify the date of news regarding Brexit announcements (red bars) and monetary policy activities. The latter have been divided into interest rate announcements (green bars) and purchasing announcements (blue bars).

Notice how the *MVI* peaks in correspondence with the Brexit referendum, which has stormed the whole UK financial

markets by producing the highest volatility in the system. On 23 June 2016, the UK in fact voted to leave the EU, an outcome that was not considered as the main scenario by market participants. The financial markets reacted with high volatility in the days after the shock: the sterling depreciated heavily against major currencies, stock market indices in the UK decreased sharply and asset volatility increased, with volumes of trading roughly triplicate from the 23rd to the 24th of June. The VIX Index, which estimates the expected volatility of the S&P500 Index, surged from 17 to 26 in a day. This backdrop triggered a more aggressive expansionary monetary policy by the Bank of England (BoE), with interest rates cuts and additional non-standard monetary policy measures. Amid mounting signs that quitting the EU would have had an adverse impact on the UK economy, the Bank of England's Monetary Policy Committee (MPC) responded announcing on July 2016 that it would use macroprudential tools to ease credit consistently with expectations of a wider easing policy response. On August 2016, the BoE voted unanimously to reduce the benchmark rate by 25 basis points to a record-low 0.25 percent, and launched a Quantitative Easing for 170 billion pounds (223\$ billion) via purchases of gilts and corporate bonds and a lending program for banks. After that, on July 5, the BoE Financial Policy Committee decided to lower its countercyclical capital requirement to 0% from 0.5% of risk-weighted assets at least until June 2017 to improve credit intermediation and lending capacity for British banks.

As regards the UK Equity Indexes taken into consideration, in the day after the referendum the higher impact has been registered by the FTSE 250, UK's domestically focused index, that comprises medium-sized manufacturers, service companies and retailers, who are likely to be highly exposed to any UK recession more than the very large international constituents of the FTSE 100, with 75% of sales outside the UK. In fact, the FTSE250 missed the rebound of the FTSE100 in afternoon, trade London time. The FTSE100 in fact benefited from the stronger foreign revenues of the big companies included in the index, as the pound depreciates. The FTSE 250 incorporated, instead, the higher recession risk induced by the Brexit and the higher profit warnings risk for small and mid-cap stocks. The reaction overseas has been more subdued, with S&P500 contracting -3.59% .

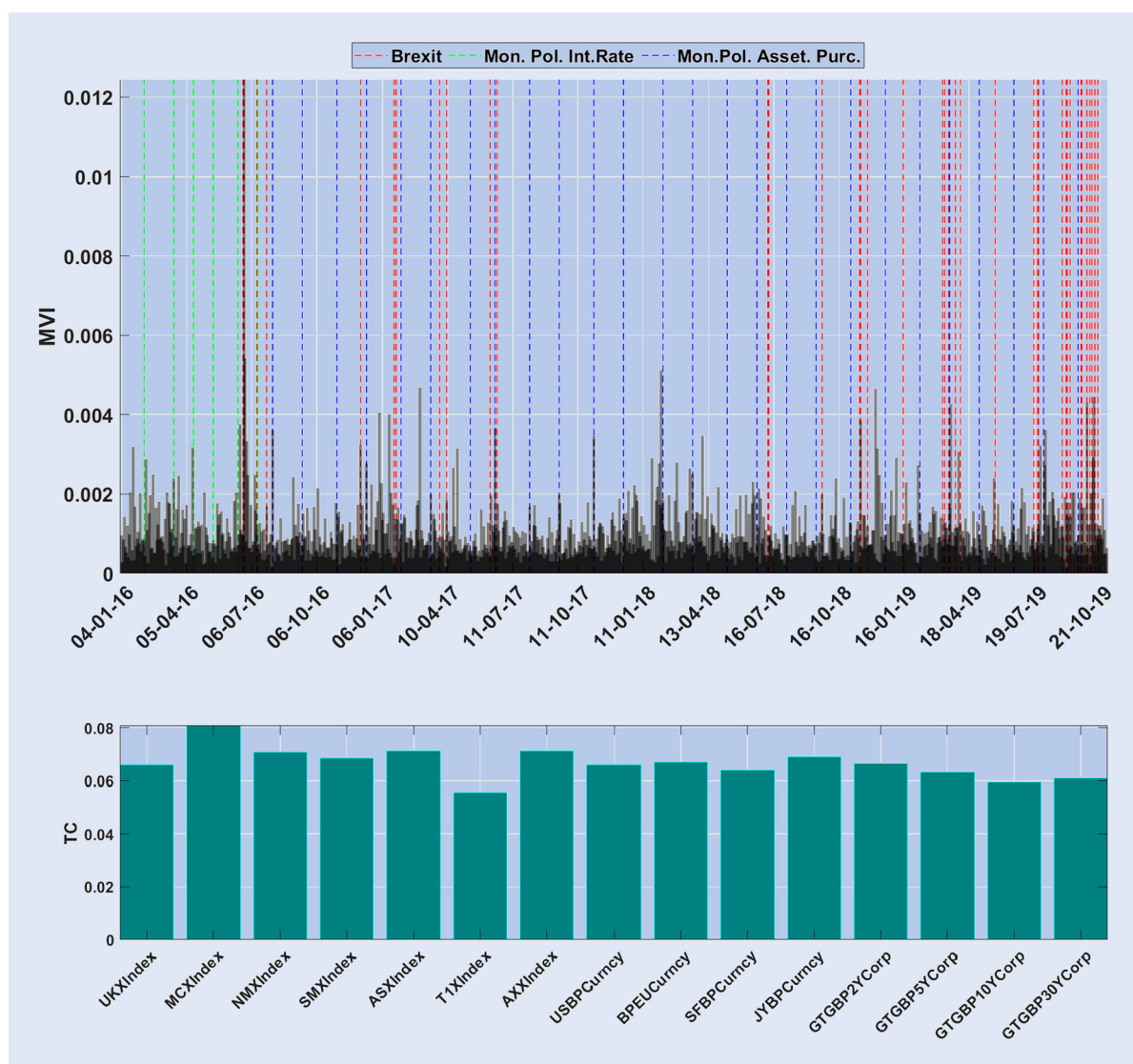


Figure 4. *MV I and type centrality scores*: Figure reports the centrality measures obtained by the probabilistic tensor decomposition. In particular, the upper panel refers to the dynamics of the *MV I* reported against the dates of Brexit-related news (red bars) and of monetary policy actions (interest rate announcements in green, and purchasing announcements, i.e. assets and corporate bonds purchase, in blue). The lower panel refers to *TC* and shows the contribution of each asset type to the value of *MV I*.

At the same time, the risk-off reaction led to a fall in Government yields, with the UK yield curve shifting downward around 30 basis point in all the maturities from 3 year to 50 years; the German curve registered a similar movement, though more tilted in the long end of the curve, while the Treasury curve saw an higher drop in the bucket 3–10 years. The Italian and Spanish curve instead moved upward, with the bucket 5–9 years that registered a 10 basis points move.

In a nutshell, the unexpected outcome of the referendum of 23 June 2016 was immediately reflected on the financial markets, mixed and varying across different sectors of Britain stock market. The main fear was that an exit without an agreement, where trade and financial ties between the world's fifth-largest economy and its biggest trading partners would collapse overnight, spreading havoc among markets and businesses. In fact, it was not clear immediately after the June 23 vote what form the new trade regime between the UK and the EU or the rest of the world would take: the best case was the so-called 'Norwegian model' of paid access to the EU single

market, which is closest to the current UK situation. However, this option was explicitly ruled out by Prime Minister Theresa May in her 19 January 2017 speech. At the other end of the spectrum is the so-called 'hard' Brexit option, with little or no shared market access and significant restrictions on labor mobility, trade, and passporting rights.

Section A.2 of the Appendix reports the dynamics of the centrality measures for the three different asset classes under the analysis, namely the stock market in figure A1, the exchange rate market in figure A2 and the government bond market in figure A3. Specifically, we can note how the volatility of the different markets contribute to the overall *MV I* centrality of the UK financial system. Brexit announcements show an influence on UK financial system, as for instance the request to the European Council for an extension of withdrawal until 31 January 2020 wrote by Boris Jonson in 19 October 2019 which affected the sterling, and the general election held in the UK on 8 June 2017, whose effects appear visible on all the three markets. The *TC* reported on the lower

panel of figure 4, on the other hand, suggests that, on average, all the assets under analysis equally contribute to the dynamics of the MVI index, even if the MCXIndex (i.e. FTSE 250) is the series that contributes the most, while, for the government bond market, the short term (2-year) bond is the most influencing series, as expected.

3.3. The average Omori law: the impact of Brexit and monetary policy announcements

For statistically investigating the effects of the Brexit and of the monetary policy actions, we analyze the average daily variation of the MVI around the dates of the announcements by quantifying the value of the centrality measures both prior and after a market shock. In particular, in figure 5 we report the pre-shock and after-shock average cumulative distribution of the MVI before and after the main announcements together with the value of the Omori exponents for different types of announcements. Such averaging does not wash out the Omori law, but allows for better statistical estimation. We then employ a linear fit on a log–log scale to determine the Omori power-law exponents before and after the news, respectively.

In order to compare the dynamics before and after the announcements, we split the MVI dynamics symmetrically around the announcement dates. Notice that the impact of an announcement generates a power law decay of the MVI around the main dates. Interestingly, the Omori exponents are different across series (depending on the news type), thus stimulating the assessment of efficiency conditions of the corresponding market in processing different types of shocks derived from the news. In particular, we observe that the Omori exponent is positive for both the

after-shock and pre-shock cases and for both monetary policy and Brexit announcements. Moreover, the lower values of the Omori exponents related to the Brexit announcements with respect to the monetary policy actions suggest a market inefficiency in processing Brexit-related news with respect to announcements of the BoE regarding interest rates adjustments or assets purchasing. As a comparison, Petersen *et al.* (2010a, 2010b) found that, independently from the frequency of the considered time series, the announcements of the U.S. Federal Reserve about interest rates settings produce Omori exponents with magnitudes similar to those founded for the MVI and Brexit process cases, while several studies found coefficients in the range 0.2–0.3 after market crashes (see, e.g. Lillo and Mantegna 2003, 2004, Sornette *et al.* 2004, Weber *et al.* 2007). Finally, notice that between the two classes of monetary policy actions, the asset purchasing displays the highest exponent, thus suggesting more efficiency levels in processing information. More generally, this can be due to the fact that the dates of the purchasing and the quantity of purchased assets by the BoE are known in advance by market participants. In Section A.3, we replicate our analysis but looking separately at the three asset classes that compose the aggregate UK financial system; results hold for all the three classes, supporting the presence of some degree of market inefficiency in processing Brexit-related news when compared to monetary policy announcements.

3.4. The Omori exponent for single Brexit events: discounted and unexpected announcements

Despite Section 3.3 provides useful insights on the average effect of Brexit-related news on the aggregate UK financial system volatility by allowing a comparison with monetary policy announcements, the aggregation procedure prevents a deep investigation of the effects of each single event on MVI values.

For this purpose, in this section we report the Omori exponents (β_{MVI}) related to each single Brexit announcement for both the pre- and after-shock cases. Notice in figure 6 the existence of negative exponents that we can interpret as fully discounted news if the exponent is related to the pre-shock case, or as an unexpected news if the negative exponent is referring to the after-shock case. Indeed, the negative exponents in the case of pre-shock correspond to MVI values in which the pre-shocks farther away from the announcement date are dominant over the volatility cascade around time $\tau = 0$, while the negative exponent in the case of after-shock corresponds to MVI values that peak after the date of the announcement, thus suggesting an unexpected announcement from the market. This is especially true, in the pre-shock case, for the event corresponding to the 19 October 2019, when news were fully discounted by the markets. At that date a special Saturday sitting of Parliament was held to debate the revised withdrawal agreement and delaying consideration of the agreement until the legislation to implement passed.

On the contrary, markets were surprised by the 3 September 2019 news, when took place a motion for an emergency

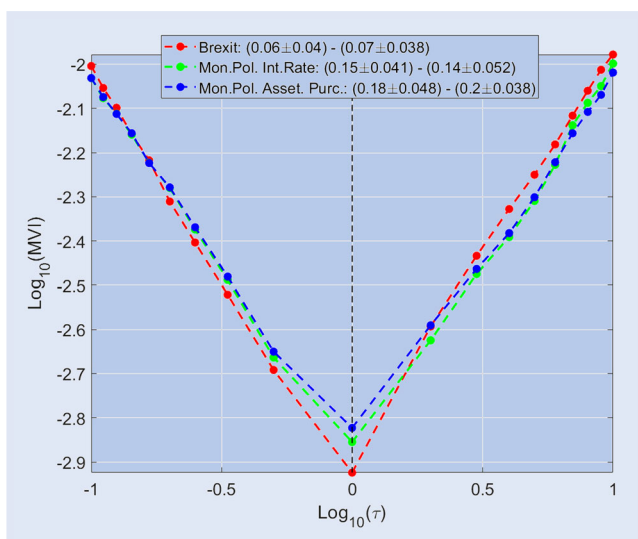


Figure 5. *Omori relationships*: Figure reports the log–log plot of the average cumulative distribution function of the MVI around the days of the external shocks. Lines are reported with different colors, Brexit events are displayed in red, while interest rate interventions are shown in green and monetary policy actions of assets purchasing in blue. The legend provides the value of the Omori exponent for both pre-shocks and after-shocks.

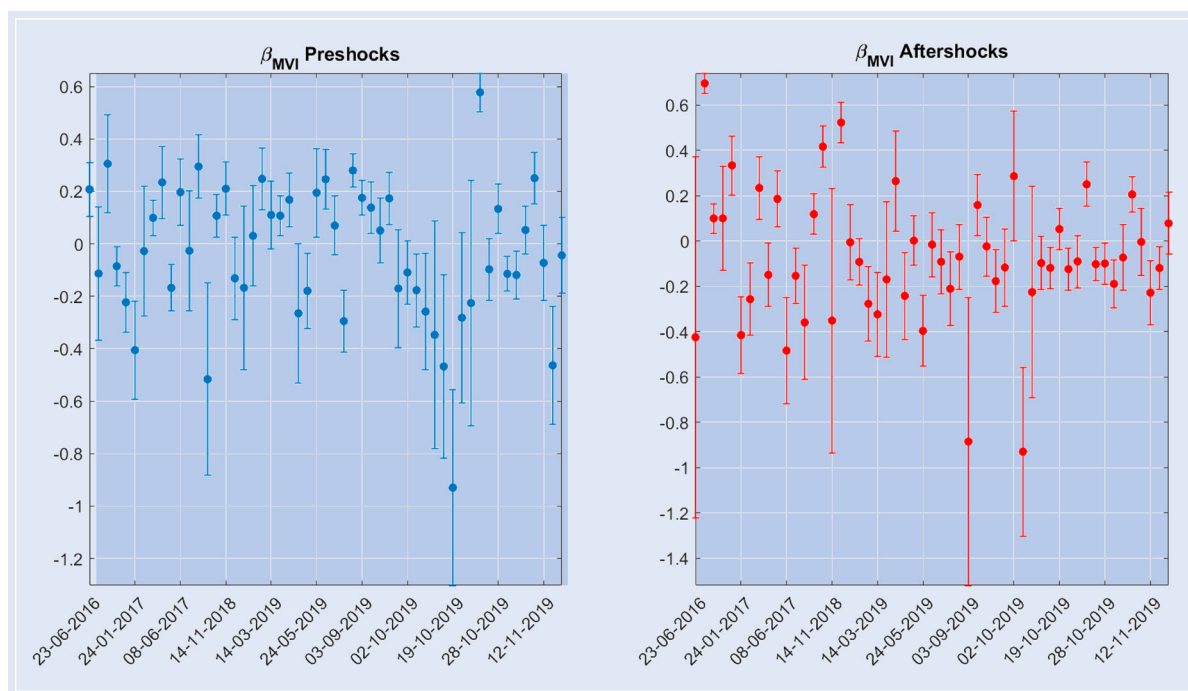


Figure 6. *Omori relationships by single Brexit announcements*: Figure reports Omori exponents related to the cumulative distribution function of the *MVI* around single dates of the Brexit announcements. The left panel refers to the pre-shock case, while the right panel shows the exponents for the after-shock case.

debate that would rule out a unilateral no-deal Brexit by forcing the Government to get parliamentary approval for either a withdrawal agreement or a no-deal Brexit. Another example is the 7 October 2019, when the Outer House of the Court of Session in Edinburgh dismisses a case brought by petitioners seeking a court order compelling Boris Johnson to write the letter requesting an extension that could be required by the Benn Act.

In Section A.4 of the Appendix, we report the achieved results for the three different asset classes. Also in this case we found that some peculiar announcements were fully discounted by the market, while others, on the contrary, were unexpected by market participants thus creating a surprise effect in the system.

4. Conclusion

In this paper, we have proposed a multi-layer visibility network approach to depict the dynamic response of the UK financial system's volatility to both the main Brexit-related news and BoE monetary policy announcements. To study the impacts of the Brexit process on the UK financial system, we have considered the main equity indexes, government interest rates and cross currency rates against Sterling, over the 3-year period 2016–2019. Moreover, in order to map the UK financial system's volatility, we have detected the dates of the occurrences of key events in the Brexit path from referendum to the EU exit agreement.

More specifically, we had been able to quantify both in temporal and cross-sectional dimensions the magnitude and co-movement among volatility series, by decomposing a visibility multi-layer network. Studying the statistical properties

of the resulting centrality measures, we have quantified how external news related to the Brexit process induced 'after-shocks' and 'pre-shocks' to the system.

We have found the effects on equity and bond markets were evident after the unexpected result of the Brexit referendum. The phase of risk-off generated by the referendum has led to a preference for safe haven assets, UK government rates have been impacted in a softer manner, and, in particular, long yields have remained anchored thanks to the expansionary stance of the BoE and supported by all the main Central Banks. Corporate bonds, both investment grade and high yield, have been impacted and the spread over Gilts surged.

Moreover, our analysis has revealed that the UK financial system under-reacted to the Brexit news by taking a finite time to adjust prices to pre-shock levels, thus moving against the efficient market hypothesis. Indeed, we have empirically observed lower values of the Omori exponents related to the Brexit announcements than to the monetary policy actions. We can interpret this finding as market inefficiency in processing Brexit-related news relative to announcements of the BoE regarding interest rate adjustments or asset purchasing.

We have intentionally excluded the behavior of the market in 2020, since it has been severely impacted by the Covid-19 shock, that caused high volatility behavior and drawdowns that had no precedent for speed and harshness, followed by a recession induced by the lockdown measures implemented to fight the Covid-19 spread, which has lead the Bank of England to a drastic change in the way it implements policy, with all the policy tools—bank rate, balance sheet, and forward guidance—deployed simultaneously. Future studies may incorporate such dynamics as well as the extension to high frequency data to map market response in an even more timely way.

Disclosure statement

No potential conflict of interest was reported by the author(s).

ORCID

Maria Elena De Giuli  <http://orcid.org/0000-0002-5221-0005>

References

- Aldasoro, I. and Alves, I., Multiplex interbank networks and systemic importance: An application to European data. *J. Financ. Stability*, 2018, **35**, 17–37.
- Armour, J., Brexit and financial services. *Oxford Rev. Economic Policy*, 2017, **33**(suppl_1), S54–S69.
- Avdjiev, S., Giudici, P. and Spelta, A., Measuring contagion risk in international banking. *J. Financ. Stability*, 2019, **42**, 36–51.
- Barberis, N., Shleifer, A. and Vishny, R., A model of investor sentiment. *J. Financ. Econ.*, 1998, **49**(3), 307–343.
- Belke, A., Dubova, I. and Osowski, T., Policy uncertainty and international financial markets: The case of Brexit. *Appl. Econ.*, 2018, **50**(34–35), 3752–3770.
- Borghesi, S. and Flori, A., With or without UK: A pre-Brexit network analysis of the EU ets. *PLoS ONE*, 2019, **14**(9), e0221587.
- Campanharo, A.S., Sire, M.I., Malmgren, R.D., Ramos, F.M. and Amaral, L.A.N., Duality between time series and networks. *PLoS ONE.*, 2011, **6**(8), e23378.
- Corsetti, G., Crowley, M., Han, L. and Song, H., Markets and markup: A new empirical framework and evidence on exporters from China, 2019.
- Ding, Z., Granger, C.W. and Engle, R.F., A long memory property of stock market returns and a new model. *J. Empir. Financ.*, 1993, **1**(1), 83–106.
- Donner, R.V., Small, M., Donges, J.F., Marwan, N., Zou, Y., Xiang, R. and Kurths, J., Recurrence-based time series analysis by means of complex network methods. *Int. J. Bifurcat. Chaos*, 2011, **21**(04), 1019–1046.
- Donner, R.V., Zou, Y., Donges, J.F., Marwan, N. and Kurths, J., Recurrence networks—A novel paradigm for nonlinear time series analysis. *New. J. Phys.*, 2010, **12**(3), 033025.
- Driffield, N. and Karoglou, M., Brexit and foreign investment in the UK. *J. R. Stat. Soc.: Ser A (Stat. Soc.)*, 2019, **182**(2), 559–582.
- Fama, E.F., The behavior of stock-market prices. *J. Business*, 1965, **38**(1), 34–105.
- Flori, A., Pammolli, F., Buldyrev, S.V., Regis, L. and Stanley, H.E., Communities and regularities in the behavior of investment fund managers. *Proc. Natl. Acad. Sci.*, 2019, **116**(14), 6569–6574.
- Flori, A., Pammolli, F. and Spelta, A., Commodity prices comovements and financial stability: A multidimensional visibility nexus with climate conditions. *J. Financ. Stability*, 2021, **54**, 100876.
- Gauvin, L., Panisson, A. and Cattuto, C., Detecting the community structure and activity patterns of temporal networks: A non-negative tensor factorization approach. *PLoS ONE.*, 2014, **9**(1), e86028.
- Gonçalves, B.A., Carpi, L., Rosso, O.A. and Ravetti, M.G., Time series characterization via horizontal visibility graph and information theory. *Phys. A: Stat. Mech. Appl.*, 2016, **464**, 93–102.
- Haraguchi, Y., Shimada, Y., Ikeguchi, T. and Aihara, K., Transformation from complex networks to time series using classical multidimensional scaling. In *International Conference on Artificial Neural Networks*, pp. 325–334, 2009 (Springer: Heidelberg).
- Hastie, T., Tibshirani, R. and Friedman, J., *The Elements of Statistical Learning: Prediction, Inference and Data Mining*, 2009 (Springer-Verlag: New York).
- Heemeijer, P., Hommes, C., Sonnemans, J. and Tuinstra, J., Price stability and volatility in markets with positive and negative expectations feedback: An experimental investigation. *J. Econ. Dyn. Control*, 2009, **33**(5), 1052–1072.
- Hosoe, N., Impact of border barriers, returning migrants, and trade diversion in Brexit: Firm exit and loss of variety. *Econ. Model.*, 2018, **69**, 193–204.
- Jackson, K. and Shepotylo, O., Post-Brexit trade survival: Looking beyond the union. *Econ. Model.*, 2018, **73**, 317–328.
- Kantz, H. and Schreiber, T., *Nonlinear Time Series Analysis*, Vol. 7, 2004 (Cambridge University Press).
- Kleinberg, J.M., Authoritative sources in a hyperlinked environment. *J. ACM (JACM)*, 1999, **46**(5), 604–632.
- Kolda, T.G. and Bader, B.W., Tensor decompositions and applications. *SIAM Rev.*, 2009, **51**(3), 455–500.
- Kolda, T.G., Bader, B.W. and Kenny, J.P., Higher-order web link analysis using multilinear algebra. In *Proceedings of the Fifth IEEE International Conference on Data Mining (ICDM'05)*, pp. 242–249, 2005 (IEEE: Washington, DC).
- Lacasa, L. and Flanagan, R., Time reversibility from visibility graphs of nonstationary processes. *Phys. Rev. E.*, 2015, **92**(2), 022817.
- Lacasa, L., Luque, B., Ballesteros, F., Luque, J. and Nuno, J.C., From time series to complex networks: The visibility graph. *Proc. Natl. Acad. Sci.*, 2008, **105**(13), 4972–4975.
- Lacasa, L., Luque, B., Luque, J. and Nuno, J.C., The visibility graph: A new method for estimating the hurst exponent of fractional Brownian motion. *EPL (Europhys. Lett.)*, 2009, **86**(3), 30001.
- Lacasa, L., Nicosia, V. and Latora, V., Network structure of multivariate time series. *Sci. Rep.*, 2015, **5**, 15508.
- Li, H., Volatility spillovers across European stock markets under the uncertainty of Brexit. *Econ. Model.*, 2019, **84**, 1–12.
- Lillo, F. and Mantegna, R.N., Power-law relaxation in a complex system: Omori law after a financial market crash. *Phys. Rev. E.*, 2003, **68**(1), 016119.
- Lillo, F. and Mantegna, R.N., Dynamics of a financial market index after a crash. *Phys. A: Stat. Mech. Appl.*, 2004, **338**(1–2), 125–134.
- Mandelbrot, B.B., The variation of certain speculative prices. In *Fractals and Scaling in Finance*, pp. 371–418, 1997 (Springer: New York).
- Mantegna, R.N. and Stanley, H.E., *Introduction to Econophysics: Correlations and Complexity in Finance*, 1999 (Cambridge University Press).
- Menkhoff, L., Rebitzky, R.R. and Schröder, M., Heterogeneity in exchange rate expectations: Evidence on the chartist–fundamentalist approach. *J. Econ. Behav. Organ.*, 2009, **70**(1–2), 241–252.
- Montagna, M. and Kok, C., Multi-layered interbank model for assessing systemic risk, 2016.
- Ng, M. K.-P., Li, X. and Ye, Y., MultiRank: Co-ranking for objects and relations in multi-relational data. In *The 17th ACM SIGKDD Conference on Knowledge Discovery and Data Mining (KDD-2011), August 21–24*, pp. 1217–1225, 2011 (ACM: San Diego, CA).
- Nowak, S., Andritzky, J., Jobst, A. and Tamirisa, N., Macroeconomic fundamentals, price discovery, and volatility dynamics in emerging bond markets. *J. Bank. Financ.*, 2011, **35**(10), 2584–2597.
- Omori, F., On the aftershocks of earthquakes. *J. College Sci.*, 1894, **7**, 111–200.
- Pagnottoni, P., Spelta, A., Pecora, N., Flori, A. and Pammolli, F., Financial earthquakes: Sars-cov-2 news shock propagation in stock and sovereign bond markets. *Phys. A: Stat. Mech. Appl.*, 2021, **582**, 126240.
- Pain, N. and Young, G., The macroeconomic impact of UK withdrawal from the EU. *Econ. Model.*, 2004, **21**(3), 387–408.
- Pecora, N. and Spelta, A., A multi-way analysis of international bilateral claims. *Soc. Networks.*, 2017, **49**, 81–92.
- Petersen, A.M., Wang, F., Havlin, S. and Stanley, H.E., Market dynamics immediately before and after financial shocks: Quantifying the Omori, productivity, and bath laws. *Phys. Rev. E.*, 2010a, **82**(3), 036114.

- Petersen, A.M., Wang, F., Havlin, S. and Stanley, H.E., Quantitative law describing market dynamics before and after interest-rate change. *Phys. Rev. E.*, 2010b, **81**(6), 066121.
- Poledna, S., Molina-Borboa, J.L., Martínez-Jaramillo, S., Van Der Leij, M. and Thurner, S., The multi-layer network nature of systemic risk and its implications for the costs of financial crises. *J. Financ. Stability*, 2015, **20**, 70–81.
- Ramiah, V., Pham, H.N. and Moosa, I., The sectoral effects of Brexit on the British economy: Early evidence from the reaction of the stock market. *Appl. Econ.*, 2017, **49**(26), 2508–2514.
- Samitas, A., Polyzos, S. and Siriopoulos, C., Brexit and financial stability: An agent-based simulation. *Econ. Model.*, 2018, **69**, 181–192.
- Schiereck, D., Kiesel, F. and Kolaric, S., Brexit: (Not) another Lehman moment for banks?. *Finance Res. Lett.*, 2016, **19**, 291–297.
- Selçuk, F., Financial earthquakes, aftershocks and scaling in emerging stock markets. *Phys. A: Stat. Mech. Appl.*, 2004, **333**, 306–316.
- Selçuk, F. and Gençay, R., Intraday dynamics of stock market returns and volatility. *Phys. A: Stat. Mech. Appl.*, 2006, **367**, 375–387.
- Serafino, M., Gabrielli, A., Caldarelli, G. and Cimini, G., Statistical validation of financial time series via visibility graph. Preprint [arXiv:1710.10980](https://arxiv.org/abs/1710.10980), 2017.
- Shahzad, K., Rubbaniy, G., Lensvelt, M. and Bhatti, T., UK's stock market reaction to Brexit process: A tale of two halves. *Econ. Model.*, 2019, **80**, 275–283.
- Shirazi, A., Jafari, G.R., Davoudi, J., Peinke, J., Tabar, M.R.R. and Sahimi, M., Mapping stochastic processes onto complex networks. *J. Stat. Mech.: Theory Experi.*, 2009, **2009**(07), P07046.
- Siokis, F.M., The dynamics of a complex system: The exchange rate crisis in southeast asia. *Econ. Lett.*, 2012, **114**(1), 98–101.
- Sornette, D., Johansen, A. and Bouchaud, J.-P., Stock market crashes, precursors and replicas. *J. De Phys. I*, 1996, **6**(1), 167–175.
- Sornette, D., Malevergne, Y. and Muzy, J.-F., Volatility fingerprints of large shocks: Endogenous versus exogenous. In *The Application of Econophysics*, pp. 91–102, 2004 (Springer: Tokyo).
- Spelta, A., Financial market predictability with tensor decomposition and links forecast. *Appl. Netw. Sci.*, 2017, **2**(1), 7.
- Spelta, A., Flori, A. and Pammolli, F., Investment communities: Behavioral attitudes and economic dynamics. *Soc. Networks.*, 2018, **55**, 170–188.
- Spelta, A., Flori, A., Pecora, N., Buldyrev, S. and Pammolli, F., A behavioral approach to instability pathways in financial markets. *Nat. Commun.*, 2020, **11**(1), 1–9.
- Spelta, A., Pecora, N., Flori, A. and Giudici, P., The impact of the sars-cov-2 pandemic on financial markets: A seismologic approach. *Ann. Oper. Res.*, 2021, 1–26.
- Stephen, M., Gu, C. and Yang, H., Visibility graph based time series analysis. *PLoS ONE*, 2015, **10**(11), e0143015.
- Strozzi, F., Zaldívar, J.-M., Poljanšek, K., Bono, F. and Gutierrez, E., *From Complex Networks to Time Series Analysis and Viceversa: Application to Metabolic Networks*, 2009 (Citeseer).
- Utsu, T., A statistical study on the occurrence of aftershocks. *Geophys. Magaz.*, 1961, **30**, 521–605.
- Vasilopoulou, S., Uk euroscepticism and the Brexit referendum. *Polit. Q.*, 2016, **87**(2), 219–227.
- Weber, P., Wang, F., Vodenska-Chitkushev, I., Havlin, S. and Stanley, H.E., Relation between volatility correlations in financial markets and Omori processes occurring on all scales. *Phys. Rev. E.*, 2007, **76**(1), 016109.
- Xu, X., Zhang, J. and Small, M., Superfamily phenomena and motifs of networks induced from time series. *Proc. Natl. Acad. Sci.*, 2008, **105**(50), 19601–19605.
- Zhang, J. and Small, M., Complex network from pseudoperiodic time series: Topology versus dynamics. *Phys. Rev. Lett.*, 2006, **96**(23), 238701.

Appendix

A.1. Main events and dates of the Brexit process

Brexit Events		Monerary Policy Events	
2016		2016	
February 22, 2016	Referendum date announced	January 14, 2016	Bank rate decision
June 23, 2016	Polling day for the EU referendum	February 4, 2016	Bank rate decision
June 24, 2016	Cameron announces resignation	March 17, 2016	Bank rate decision
July 11, 2016	Theresa May wins the Conservative Party leadership	April 14, 2016	Bank rate decision
July 13, 2016	Theresa May new PM	May 12, 2016	Bank rate decision
July 27, 2016	Michel Barnier is named as the EU's Chief Negotiator	June 16, 2016	Bank rate decision
December 7, 2016	The House of Commons vote on respecting the outcome of the referendum	July 14, 2016	Bank rate decision
		August 4, 2016	Bank rate decision
		November 3, 2016	Bank rate decision asset purchase
		December 15, 2016	Bank rate decision asset purchase
2017		2017	
January 17, 2017	May sets out plan for Brexit	February 2, 2017	Bank rate decision asset purchase
January 24, 2017	Supreme Court delivers on Article 50	March 16, 2017	Bank rate decision asset purchase
January 27, 2017	Government publishes European Union (Notification of Withdrawal) Bill	May 11, 2017	Bank rate decision asset purchase
January 31, 2017	Parliament debate on Article 50	June 15, 2017	Bank rate decision asset purchase
February 1, 2017	MPs vote on the Brexit bill	August 3, 2017	Bank rate decision asset purchase
February 2, 2017	White paper on Brexit	September 14, 2017	Bank rate decision asset purchase
February 7, 2017	MPs call for final approval on EU deal	November 2, 2017	Bank rate decision asset purchase
March 27, 2017	European Union (Notification of Withdrawal) Act received Royal Assent	December 14, 2017	Bank rate decision asset purchase
March 29, 2017	Article 50 triggered at last		
April 6, 2017	Theresa May meets with Donald Tusk		
April 18, 2017	Snap elections announced		
April 29, 2017	First Brexit summit for EU leaders		
June 8, 2017	Snap general election, May loses majority		
July 6, 2017	The Cabinet meets at Chequers		
July 8, 2017	The Cabinet meets at Chequers		
June 19, 2017	First round of UK-EU exit negotiations begin		
September 22, 2017	May details Brexit stance		
2018		2018	
March 19, 2018	UK and EU agree on several key issues	February 8, 2018	Bank rate decision asset purchase
May 4, 2018	Spring 2018 Transitional Arrangements	March 22, 2018	Bank rate decision asset purchase
September 21, 2018	Theresa May gives an update on the state of the Brexit negotiations		

Brexit Events		Monerary Policy Events	
November 14, 2018	Withdrawal agreement published	May 10, 2018	Bank rate decision asset purchase
November 15, 2018	Key secretaries resign following agreement	June 21, 2018	Bank rate decision asset purchase
November 25, 2018	EU endorses withdrawal agreement	August 2, 2018	Bank rate decision asset purchase
December 11, 2018	May faces criticism from within own party	September 13, 2018	Bank rate decision asset purchase
December 17, 2018	May announces date for vote on Brexit	November 1, 2018	Bank rate decision asset purchase
		December 20, 2018	Bank rate decision asset purchase
2019		2019	
January 15, 2019	The House of Commons voted against the deal put forward by May's government	February 7, 2019	Bank rate decision asset purchase
March 12, 2019	The House of Commons again rejected the withdrawal agreement	March 21, 2019	Bank rate decision asset purchase
March 14, 2019	The government motion was passed	May 2, 2019	Bank rate decision asset purchase
March 20, 2019	May speech in Downing St	June 20, 2019	Bank rate decision asset purchase
March 21, 2019	The European Council endorsed the Instrument relating to the withdrawal agreement	August 1, 2019	Bank rate decision asset purchase
March 29, 2019	The House of Commons once again voted against the withdrawal agreement	September 19, 2019	Bank rate decision asset purchase
April 5, 2019	May sent a letter to European Council		
May 24, 2019	Theresa May announced her resignation		
July 23, 2019	Boris Johnson was elected		
July 25, 2019	EU officials reiterated once more that the Withdrawal Agreement		
August 28, 2019	Prime Minister Boris Johnson requested the prorogation of Parliament.		
September 3, 2019	Parliament returns from the Summer Recess		
September 4, 2019	PM moves a motion to hold an early General Election		
September 9, 2019	The European Union (Withdrawal) (No. 2) Act 2019 became law		
September 24, 2019	The Supreme Court of the UK ruled that the prorogue parliament was unlawful		
October 2, 2019	The Government published a fresh Brexit plan		
October 9, 2019	Preparation of the European Council		
October 10, 2019	Johnson and Varadkar led to a resumption in negotiations		
October 14, 2019	State Opening of Parliament		
October 19, 2019	Special Saturday sitting of Parliament		
October 21, 2019	The European Union (Withdrawal Agreement) Bill is introduced to Parliament		
October 22, 2019	The UK gov. brought the revised EU Withdrawal Bill to the House of Commons for debate		
October 24, 2019	Johnson demands December election, abandons 'do or die' Brexit promise		
October 29, 2019	Brexit had been delayed until 31 January		
October 30, 2019	The day named as 'exit day' in UK legislation was changed		
December 20, 2019	The European Union Bill passes its Second Reading in the House of Lords		

A.2. Centrality measures computed on different asset classes

This section is devoted to the inspection of the centrality measures obtained from the probabilistic tensor decomposition, i.e. the MVI and the TC computed separately for each asset class. In particular, figure A1 shows the MVI dynamics when only the stock market is taken into account while figure A2 refers to the exchange rate market and, finally, figure A3 shows the results for the government bond market. Notice how all the three markets have been heavily affected by the Brexit referendum showing a pronounced increase of the volatility at that date. However, the MVI computed separately for the three assets classes also shows peculiar spikes for each series. In particular, notice how for the stock market the biggest increase of the MVI index occurs in correspondence of the asset purchase announcement of the BoE in date 04 February 2018. For the exchange rate market, on the other hand, beside the Referendum announcement, another important event is the request to the European Council for an extension of withdrawal until 31 January 2020, wrote by Boris Jonson in 19 October 2019. This event has also

stormed the stock and the government bond market which was also heavily affected by the general election held in the UK on 8 June 2017.

A.3. Average Omori exponents computed on the different asset classes

In this section, we show the average MVI distribution and the related Omori exponents for three different asset classes that compose the aggregate UK financial system. In particular, figure A4 refers to the stock market, figure A5 shows the findings for the exchange rate market and figure A6 refers to the government bond market.

As for the aggregate financial system, this analysis also shows that Brexit announcements are associated with the lowest Omori exponents, both in the pre-shock and after-shock cases. Interestingly, the stock market, when compared with the other asset classes, displays on average lower exponents, while the MVI dynamics generated by Brexit announcements on the exchange rate is associated with higher

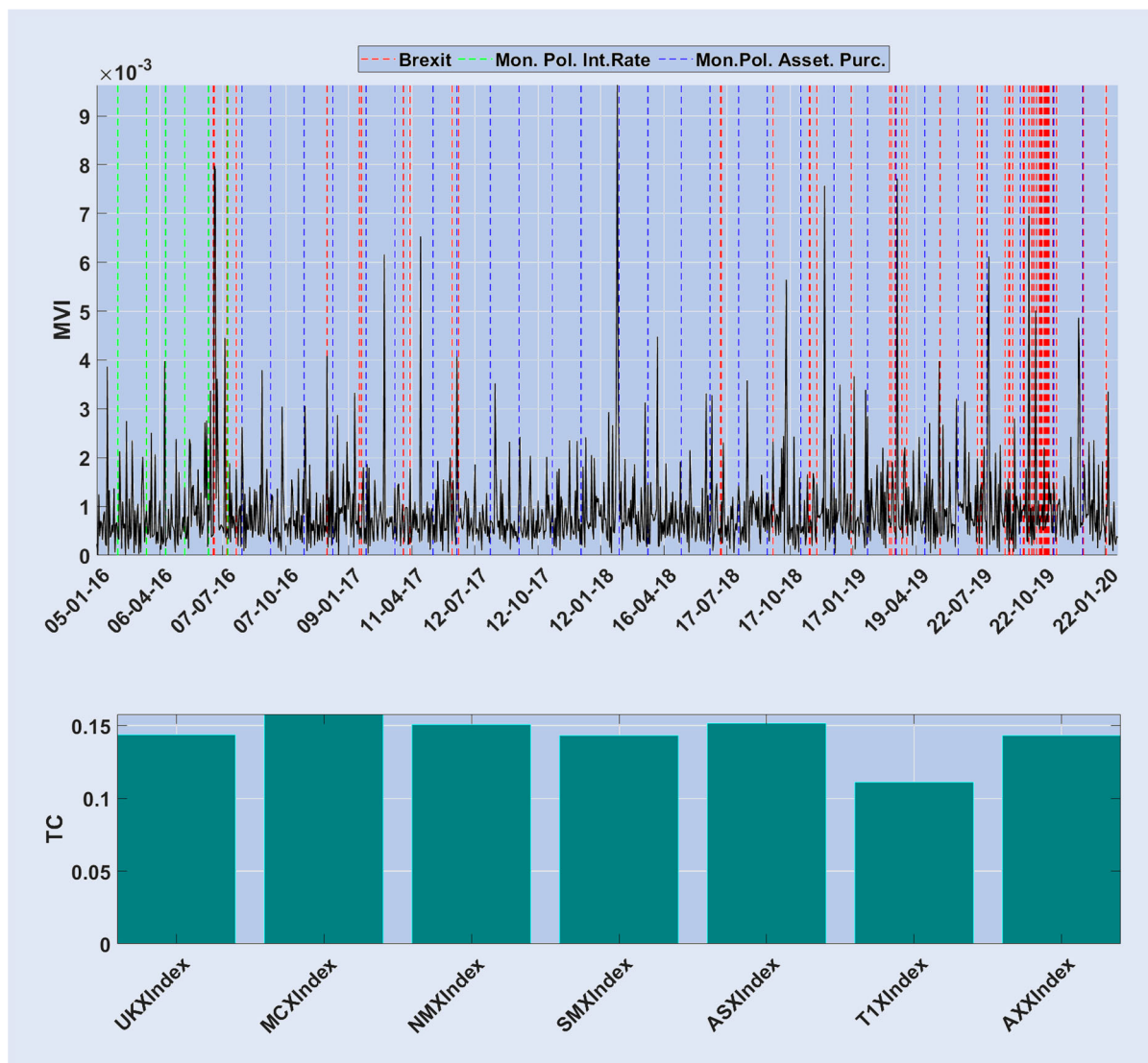


Figure A1. MVI and TC scores for the stock market: Figure reports the centrality measures obtained by the probabilistic tensor decomposition. In particular, the upper panel refers to the dynamics of the MVI reported against the dates of Brexit-related news (red bars) and of monetary policy actions (interest rate announcements in green, and purchasing announcements of assets and corporate bonds in blue). The lower panel refers to TC and shows the contribution of each asset type to the value of the MVI .

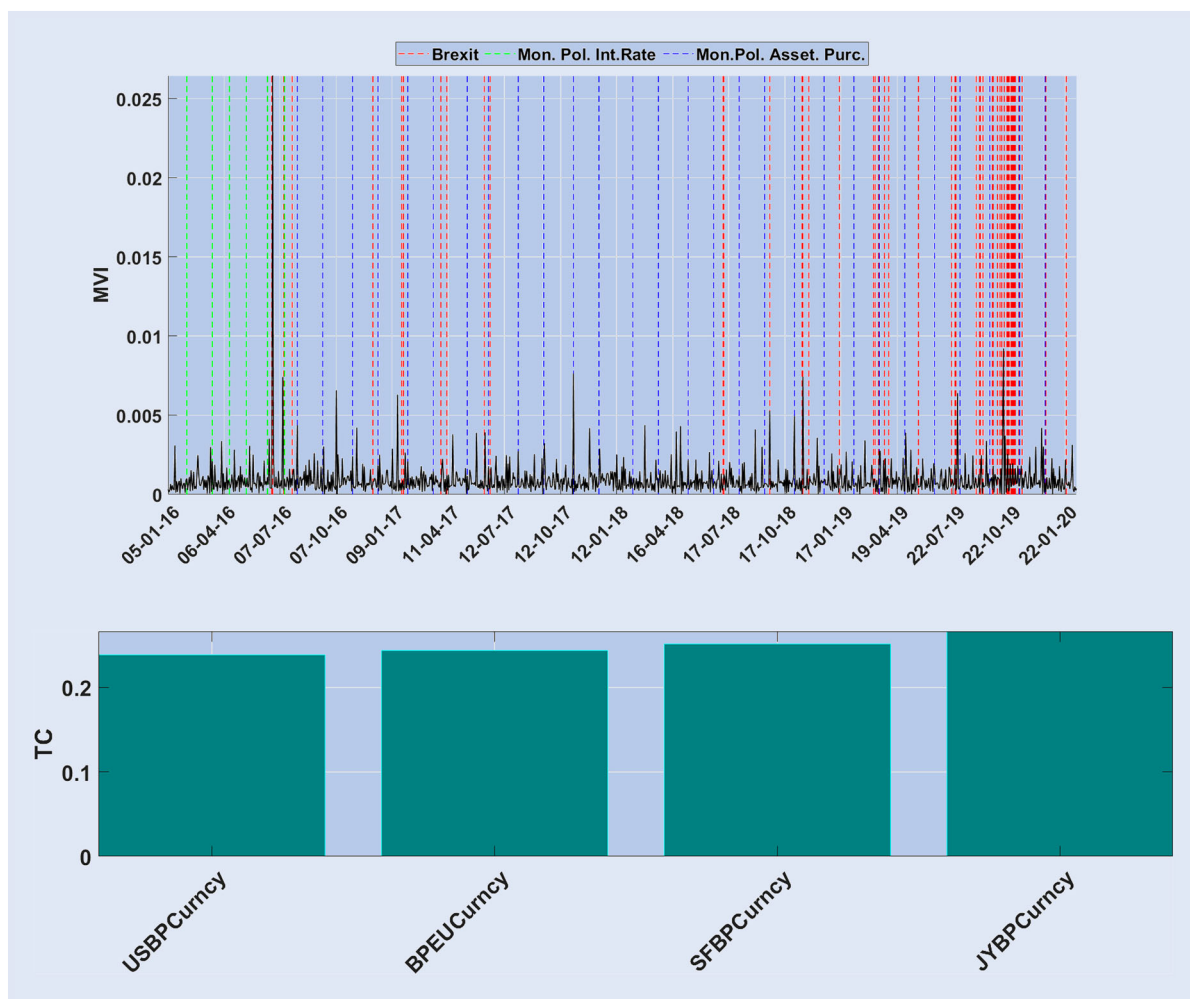


Figure A2. *MVI* and *TC* scores for the exchange rate market: Figure reports the centrality measures obtained by the probabilistic tensor decomposition. In particular, the upper panel refers to the dynamics of the *MVI* reported against the dates of Brexit-related news (red bars) and of monetary policy actions (interest rate announcements in green, and purchasing announcements of assets and corporate bonds in blue). The lower panel refers to *TC* and shows the contribution of each asset type to the value of the *MVI*.

values with respect to the ones observed on the stock and bond markets. This means that, on average, the exchange rate market is more efficient in processing Brexit related news with respect to the other asset classes.

A.4. The Omori exponent for single Brexit events computed on different asset classes

As we discuss in the main corpus of the paper, also for the analysis for each asset class we found some Brexit-related news that have been previously discounted by the market, thus having a negative Omori exponent in the pre-shock phase, and other announcements that generate a surprise effect, being unexpected by market participants and thus generating negative exponent in the after-shock case.

A.5. Volatility behavior and Omori exponents for single time series

In this Appendix section, we report the volatility dynamics computed on each single time series under analysis in figure A10 together with the relative Omori exponents in figure A11. Notice that during days of high instability, market volatility computed for the single time

series tends to be high and this market behaviour is likely to occur for many time series which leads to an increasing dynamics of *MVI*. Moreover, figure A11 shows that the Brexit announcements produce a long-lasting effect on all volatility series for which the Omori exponents in both pre- and after-shock cases are positive and, on average, statistically significant, while the effect of monetary policy announcements are assets-specific and can produce surprise effects being unexpected by market participants, thereby generating negative exponents in the after-shock case, or discounted, hence having a negative Omori exponents in the pre-shock phase.

A.6. Sensitivity analysis of the Agent-Based model

This Appendix section is devoted to illustrate the robustness of the *MVI* index to changes in the configuration parameters of the Agent-Based model (see figure A12). Here, we have to remark that the more the market volatility computed on single time series is likely to be high and the more this market behavior is likely to occur for many time series, the higher the *MVI*, which indeed signals coordinated patterns among several time series on high volatility regimes. This *MVI*'s feature that we investigate in an Agent-Based environment is maintained as long as model parameter changes as indicated by the red zones which signal high *MVI* values in correspondence of high volatility time stamps and high series' correlation.

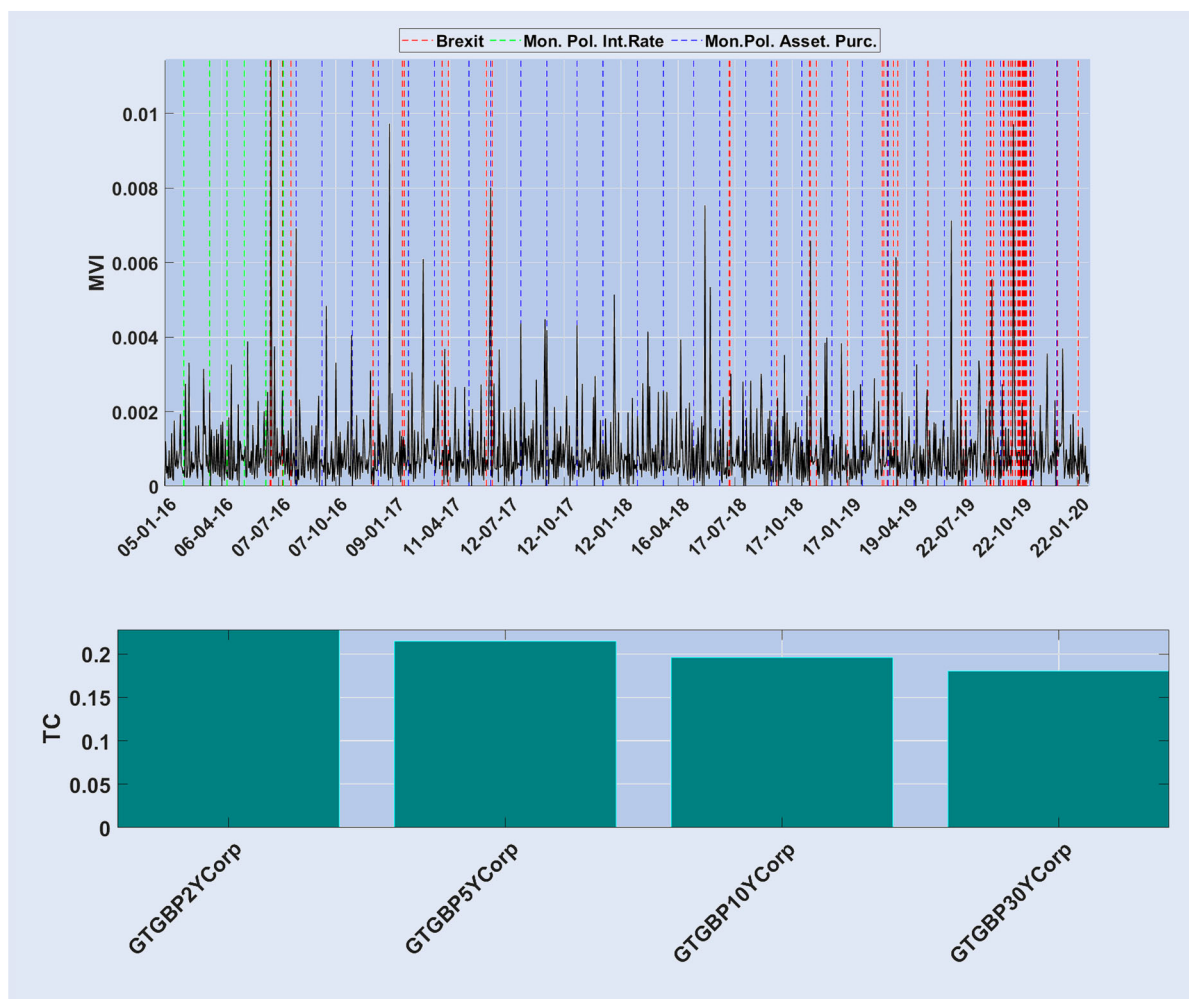


Figure A3. *MVI and TC scores for the government bond market*: Figure reports the centrality measures obtained by the probabilistic tensor decomposition. In particular, the upper panel refers to the dynamics of the *MVI* reported against the dates of Brexit-related news (red bars) and of monetary policy actions (interest rate announcements in green, and purchasing announcements of assets and corporate bonds in blue). The lower panel refers to *TC* and shows the contribution of each asset type to the value of the *MVI*.

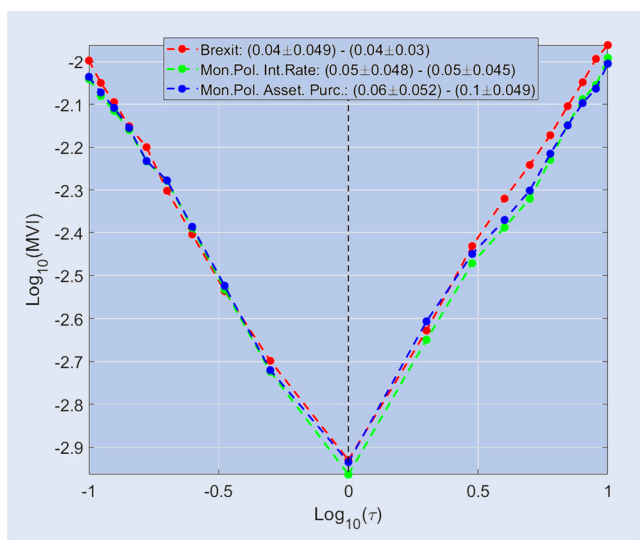


Figure A4. *Omori relationships for the stock market:* Figure reports the log–log plot of the average cumulative distribution function of the *MVI* around the days of the external shocks. Lines are reported with different colors, Brexit events are displayed in red while Interest rate interventions are shown in green and monetary policy action of assets purchasing in blue. The legend provides the value of the Omori exponent for both pre-shocks and after-shocks.

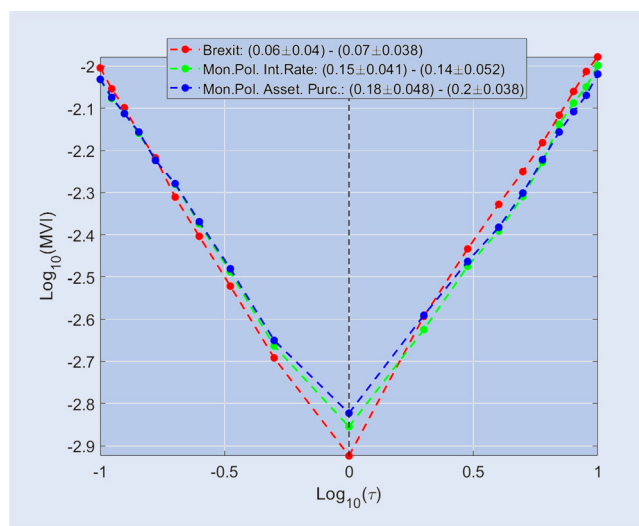


Figure A6. *Omori relationships for the government bond market:* Figure reports the log–log plot of the average cumulative distribution function of the *MVI* around the days of the external shocks. Lines are reported with different colors, Brexit events are displayed in red while interest rate interventions are shown in green and monetary policy action of assets purchasing in blue. The legend provides the value of the Omori exponent for both pre-shocks and after-shocks.

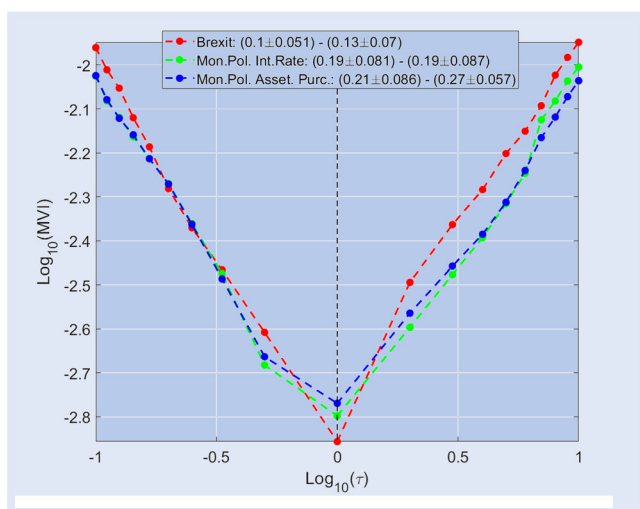


Figure A5. *Omori relationships for the exchange rate market:* Figure reports the log–log plot of the average cumulative distribution function of the *MVI* around the days of the external shocks. Lines are reported with different colors, Brexit events are displayed in red while interest rate interventions are shown in green and monetary policy action of assets purchasing in blue. The legend provides the value of the Omori exponent for both pre-shocks and after-shocks.

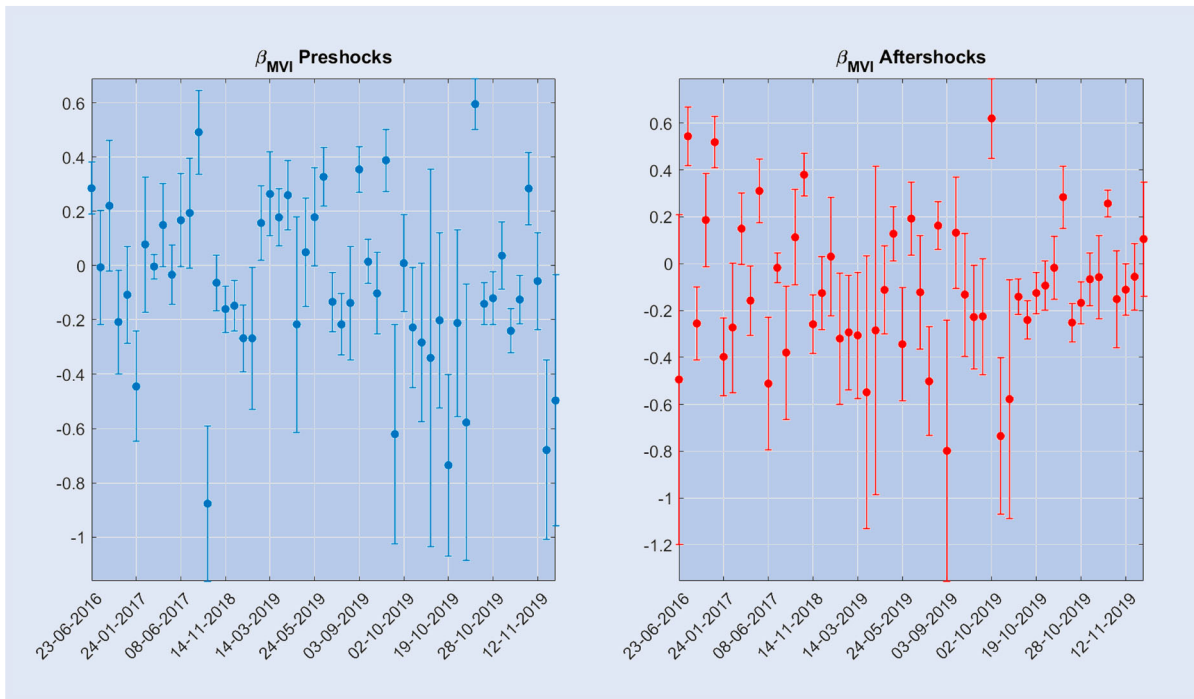


Figure A7. Omori relationships by single Brexit announcements for the stock market: Figure reports Omori exponents related to the cumulative distribution function of the *MVI* around single dates of Brexit announcements. The left panel refers to the pre-shock case while the right panel shows the exponents for the after-shock case.

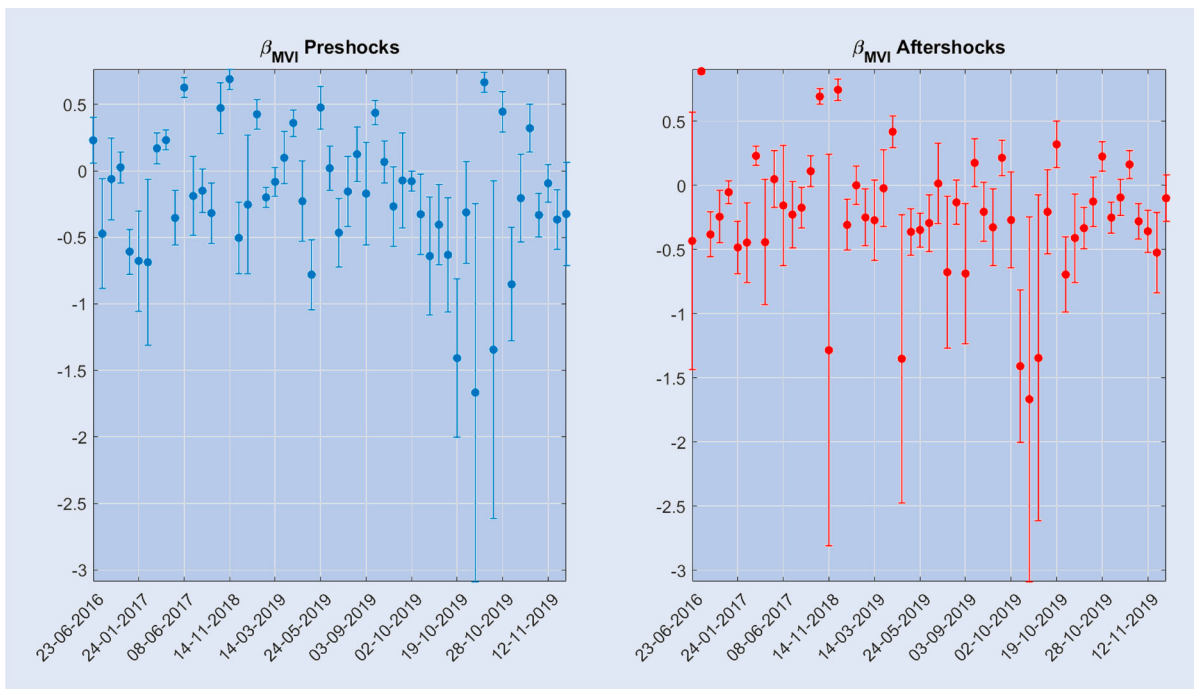


Figure A8. Omori relationships by single Brexit announcements for the exchange rate market: Figure reports Omori exponents related to the cumulative distribution function of the *MVI* around single dates of Brexit announcements. The left panel refers to the pre-shock case while the right panel shows the exponents for the after-shock case.

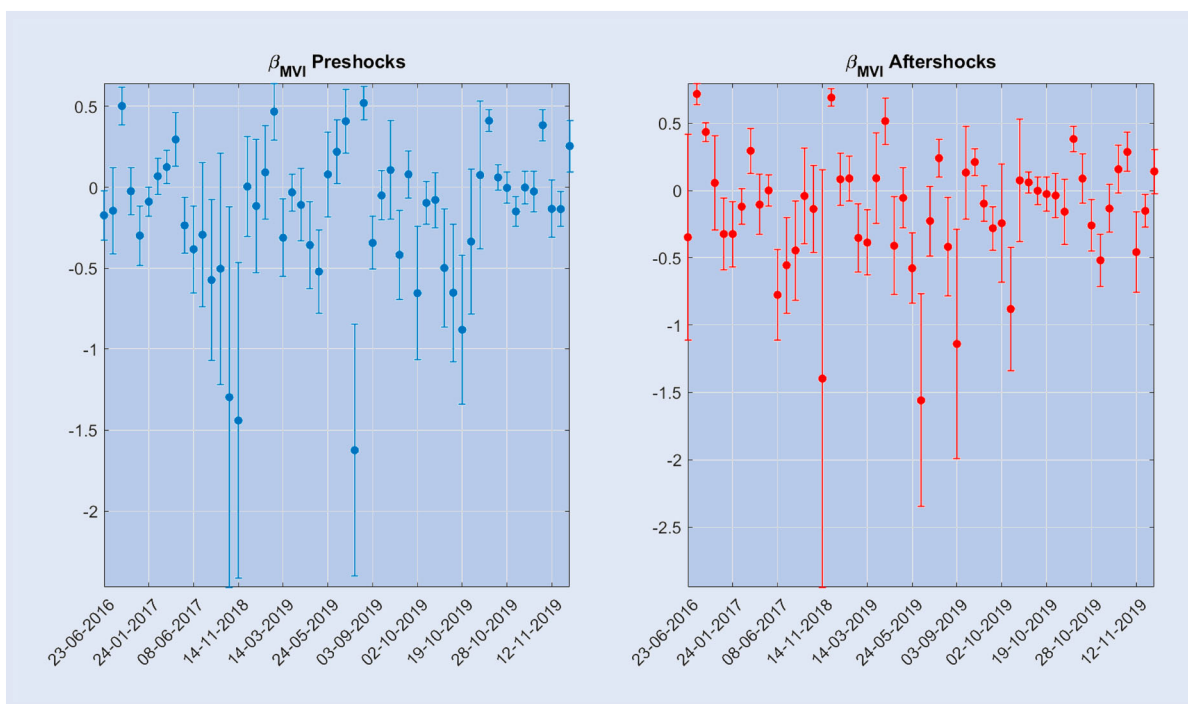


Figure A9. Omori relationships by single Brexit announcements for the government bond market: Figure reports Omori exponents related to the cumulative distribution function of the *MVI* around single dates of Brexit announcements. The left panel refers to the pre-shock case while the right panel shows the exponents for the after-shock case.

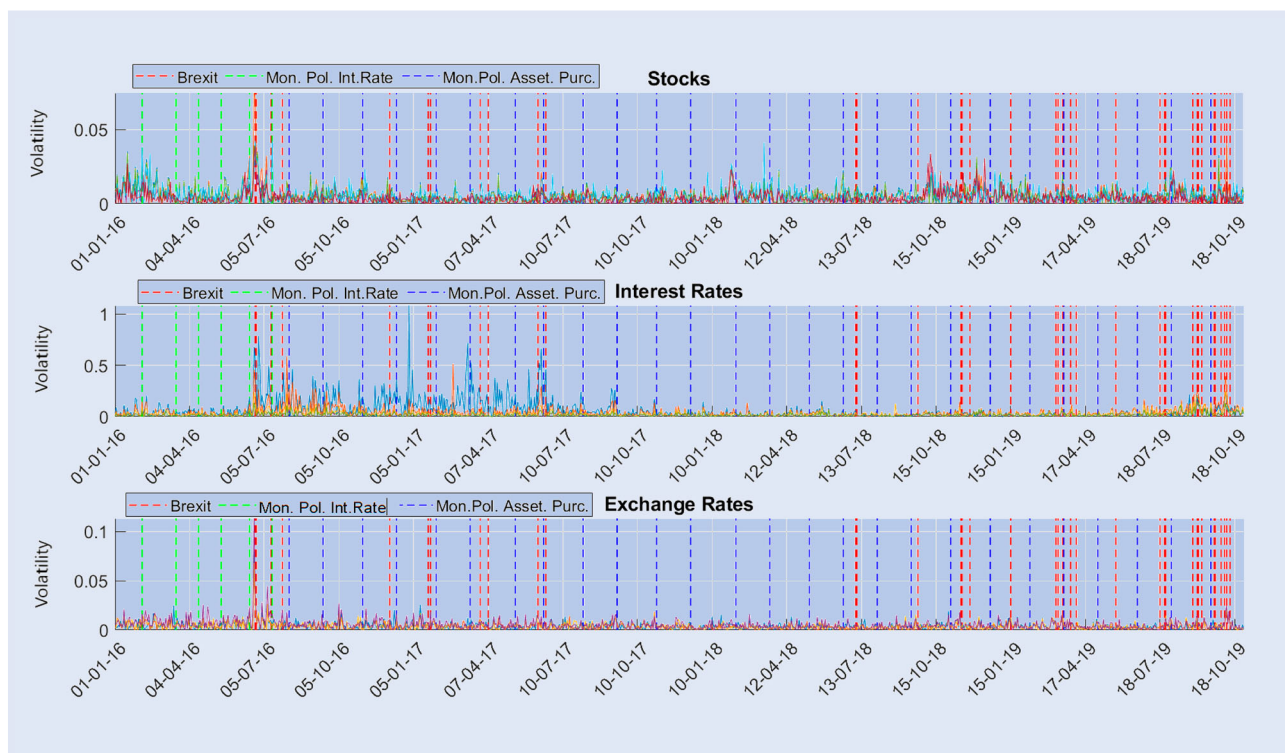


Figure A10. Time series volatility and announcement dates: Figure shows the volatility patterns for each time series, reported against the dates of Brexit-related news (red bars) and of monetary policy actions (interest rate announcements in green, and purchasing announcements of assets and corporate bonds in blue). In particular, the upper panel refers to the volatility dynamics of stock series, the central panel is dedicated to the interest rates volatility and the lower panel report the volatility of the exchange rates.

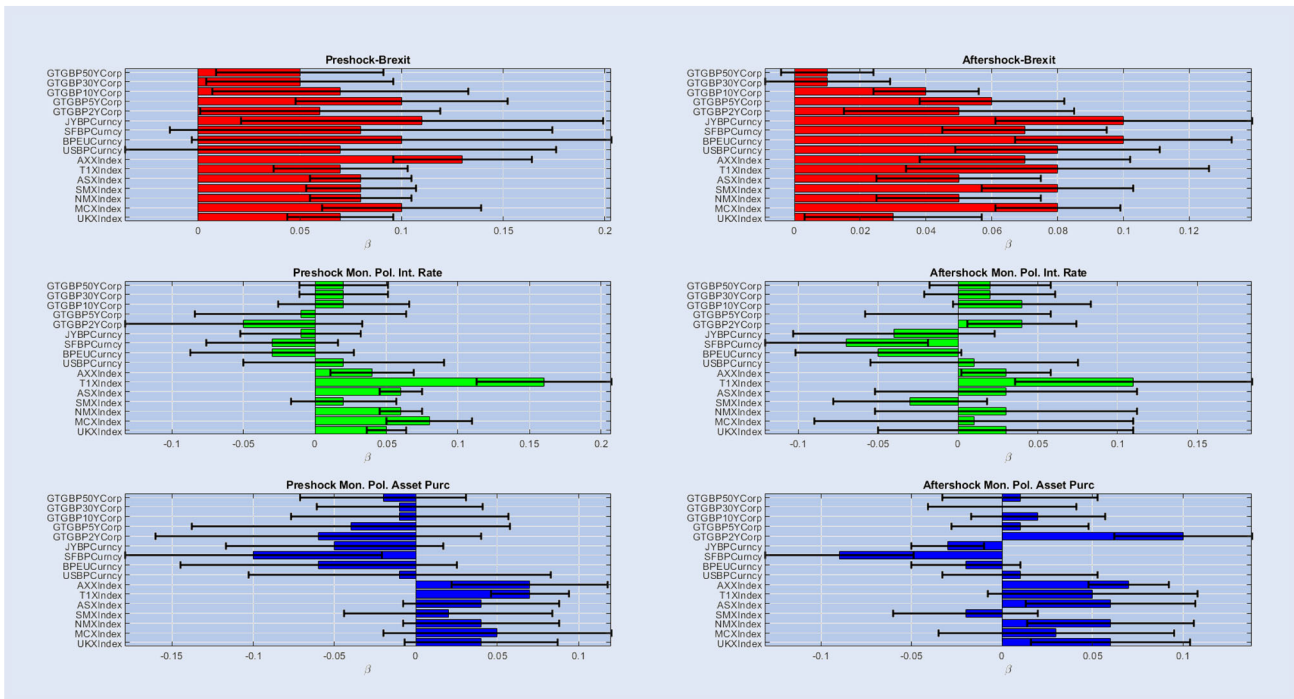


Figure A11. *Omori exponents for single times series*: Figure shows the Omori exponents computed on single times series together with confidence intervals, for the Brexit announcements (upper panel) and for interest rates (central panel) and monetary policy announcements (lower panel). Moreover, the left column refers to the pre-shock case, while the right column is dedicated to the after-shock case.

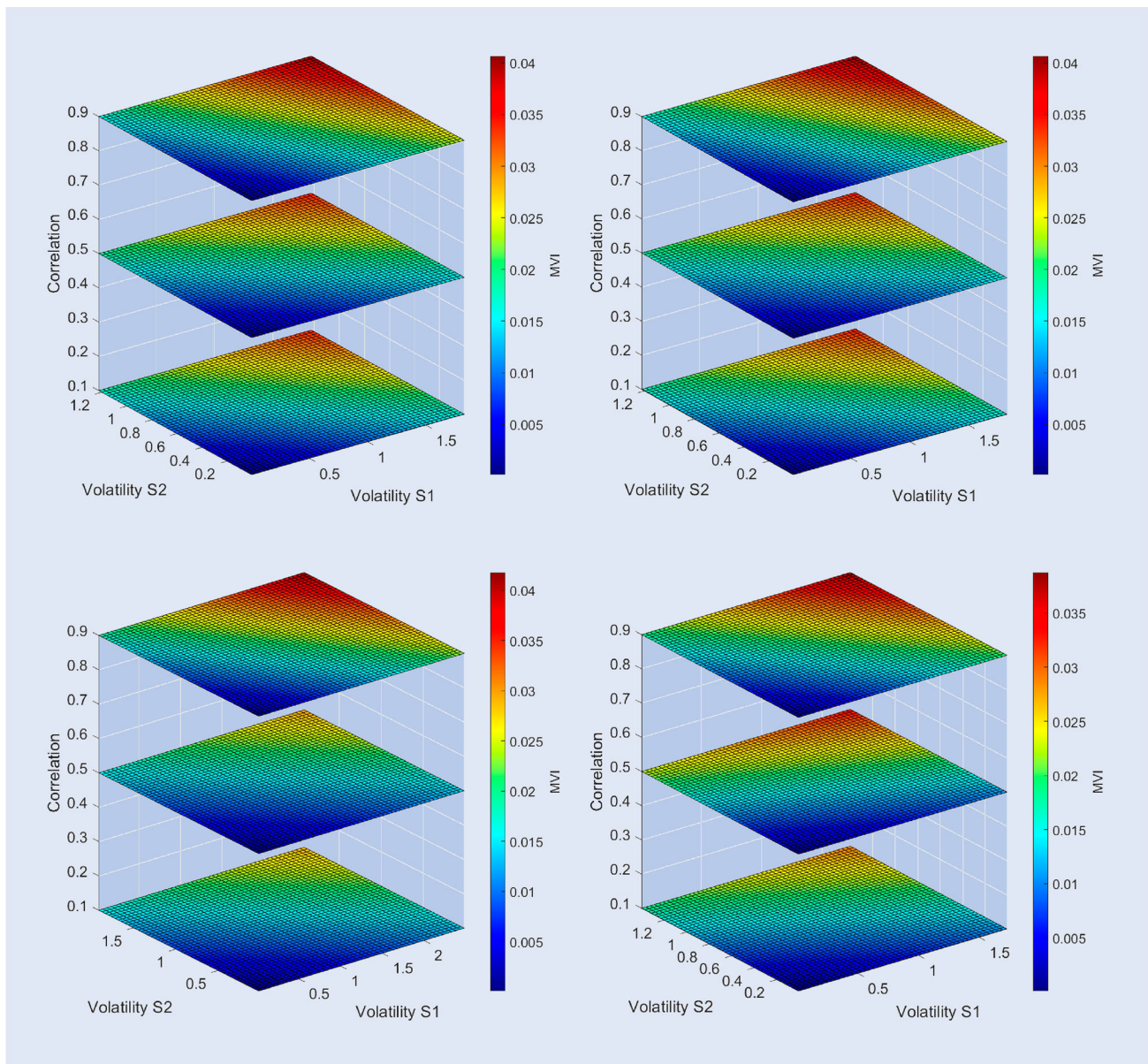


Figure A12. *Sensitivity analysis*: Figure reports *MVI* values obtained in the simulated Agent-Based model environment for different parameter combinations in the case of two time series and for different values of the correlation (0, 0.5, 0.99) of the exogenous component of the model. In particular, in the upper-left panel we set the intensity of choice parameter $e = 300$, in the upper-right panel we increase the memory parameter $d = .9$ while in the bottom panels we set the reactivity of chartists and fundamentalists to $c = .9$ and $f = .1$ in the left and $c = .1$ and $f = .9$ in the right sub-plots, respectively.